J. Fluid Mech. (2001), *vol.* 431, *pp.* 239–271. Printed in the United Kingdom

© 2001 Cambridge University Press

A multiphase model for compressible flows with interfaces, shocks, detonation waves and cavitation

By RICHARD SAUREL AND OLIVIER LEMETAYER

IUSTI, Université Aix Marseille I, 5 rue E. Fermi, 13453 Marseille Cedex 13, France *and*
INRIA, Project SMASH, Marseille, France
e-mail: richard/olimeta@iusti.univ-mrs.fr

(Received 31 January 2000 and in revised form 28 September 2000)

A compressible multiphase unconditionally hyperbolic model is proposed. It is able to deal with a wide range of applications: interfaces between compressible materials, shock waves in condensed multiphase mixtures, homogeneous two-phase flows (bubbly and droplet flows) and cavitation in liquids. Here we focus on the generalization of the formulation to an arbitrary number of fluids, and to mass and energy transfers, and extend the associated Godunov method.

We first detail the specific problems involved in the computation of thermodynamic interface variables when dealing with compressible materials separated by well-defined interfaces. We then address one of the major problems in the modelling of detonation waves in condensed energetic materials and propose a way to suppress the mixture equation of state. We then consider another problem of practical importance related to high-pressure liquid injection and associated cavitating flow. This problem involves the dynamic creation of interfaces. We show that the multiphase model is able to solve these very different problems using a unique formulation.

We then develop the Godunov method for this model. We show how the non-conservative terms must be discretized in order to fulfil the interface conditions. Numerical resolution of interface conditions and partial equilibrium multiphase mixtures also requires the introduction of infinite relaxation terms. We propose a way to solve them in the context of an arbitrary number of fluids. This is of particular importance for the development of multimaterial reactive hydrocodes. We finally extend the discretization method in the multidimensional case, and show some results and validations of the model and method.

1. Introduction

Difficult problems arise in the modelling of flows involving mixtures. These mixtures may have a physical origin as in conventional multiphase flows or may be due to numerical inaccuracies and artificial mixing as in the computation of interface variables. This occurs when an interface separates two compressible fluids of different physical properties in conjunction with the use of an Eulerian scheme.

In this introduction we review these difficulties first for flows involving fluid interfaces, then also for flows involving homogeneous mixtures, and finally for flows where interfaces appear naturally: boiling and cavitating flows. We will then develop the solution strategy valid for any of these applications.

https://doi.org/10.1017/S0022112000003098 Published online by Cambridge University Press

1.1. *Short review of methods for compressible flows with interfaces*

Compressible multifluid flows occur in many situations when fluids have different physical or thermodynamic properties and are separated by interfaces. A conventional example is an interface between air and helium under shock wave interaction. Other well-known examples are the Richtmyer–Meshkov instabilities between two gases, the behaviour of a gas bubble in a liquid in a shock wave, etc.

Many numerical simulations of such processes are based on the Euler or Navier–Stokes equations augmented by one or more species conservation equations in order to build reasonable equation of state parameters at the interface. Indeed, all conventional numerical methods produce artificial diffusion of contact discontinuities, resulting in an artificial fluid mixing at the interface. Inside this artificial mixture computation of all thermodynamic variables is inaccurate with this approach (Karni 1994; Abgrall 1996).

Frequently, the equations of state that can be found in the literature have only a limited range of validity (especially for solids and liquids). When the thermodynamic parameters provided by the numerical method are slightly outside this domain of validity, the pressure, entropy, and sound speed, that are computed have no physical meaning (negative pressure etc.). In many cases, an interface is the physical location where the flow parameters are close of the limits of validity of the equation of state. Hence a careful and clean treatment of interfaces is mandatory. Basically, two classes of methods are able to solve more or less accurately interface problems. The first class corresponds to methods where the numerical diffusion at the interfaces is eliminated. Consequently, the artificial mixing problem is eliminated too, but other practical problems may arise. The second class corresponds to methods allowing numerical diffusion at the interface and is closer to standard methods used for gas dynamics.

1.1.1. *Methods eliminating numerical diffusion at the interfaces*

(*a*) *Lagrangian methods*

In this framework the interfaces are characterized by specific positions in the flow and move with the local velocity. If the method does not use explicit artificial viscosity, the interface will remain sharp. But in fluid flows, the interface may have large deformation and the mesh suffers large distortions. These distortions are responsible for errors in the solution and it is also necessary to periodically rezone the mesh. Moreover, fluid dynamics applications deal frequently with fluid inflows and outflows. In the context of Lagrangian methods this implies addition and elimination of meshes, yielding an extra complexity. Another drawback is related to sliding lines that pose extra difficulties. An excellent review of these methods is given in Benson (1992).

(*b*) *Arbitrary Lagrangian–Eulerian* (*ALE*) *methods*

These methods are Lagrangian at the interfaces and use moving grid strategies with Eulerian schemes away from the interfaces. They allow larger distortions than strictly Lagrangian methods but are still limited. Powerful ALE methods have been developed by Farhat & Roux (1991) with a dynamic mesh management that reduces mesh distortions.

(*c*) *Front tracking methods*

These methods use a fixed grid but combine several flow solvers. Usually they use a conventional Eulerian solver for points away from the interface and a specific scheme for the points around the interface. The management of the various schemes is easy in one dimension as done for example in Harten & Hyman (1983), Mao (1993), Leveque & Shyue (1996), Cocchi & Saurel (1997). Some of these methods are strictly conservative, at least in one dimension (Harten & Hyman 1983; Leveque & Shyue

https://doi.org/10.1017/S0022112000003098 Published online by Cambridge University Press

1996). But the extension to multidimensions is no longer conservative. Actually, the main drawback is not related to the conservation, but to the interface coupling with the Eulerian scheme when the interface presents topological singularities, break-up or coalescence (Cocchi & Saurel 1997). Also, the coding of these methods, even though conceptually simple, is very difficult. In spite of these drawbacks, the accuracy of such methods is excellent in interface representation and considerable efforts have been made by specialized research teams to develop efficient three-dimensional codes (see for example Glimm *et al.* 1998).

(*d*) *Interface reconstruction methods*

Here the interfaces are not explicitly tracked but reconstructed with the help of the computation of volume fraction of the various phases. They use the VOF (volume of fluid) idea (Hirt & Nichols 1981) and reconstruction methods (Youngs 1982). These methods are widely used in hydrocodes and seem to be efficient, but certainly not conservative. They use an advection algorithm for volume fraction evolution and a reconstruction procedure to locate the interface and restore a sharp profile. Knowledge of the interface position is sufficient to determine the density field and solve the fluid dynamics equations for incompressible flows. For compressible flows, determination of the density and internal energy of each fluid in a mixed cell is not at all obvious. Papers in the literature comment very little on this point and it is not possible to evaluate these methods. However, since the applications are very important, specialized research groups have developed such codes. The published results seem to agree well with what is expected, at least for the main features of interface representation.

(*e*) *Level set methods*

The level set method (Dervieux & Thomasset 1981; Mulder, Osher & Sethian 1992) is a method used to locate fronts; it is not sufficient to compute the flow variables at an interface. But the information of the interface location may be used and combined with other ingredients to determine the flow variables. Such an idea has been proposed recently by Fedkiw *et al.* (1999) and seem to be very efficient. Although non-conservative, it allows an accurate determination of the interface characteristics and flow variables. In this method (The Ghost Fluid Method), the interface is considered as a moving boundary, and the information travels between two (or more) systems of equations by a procedure corresponding to a piston boundary condition. In order to obtain accurate results, the piston boundary condition treatment in the Euler system has been revisited and improved (Fedkiw, Marquina & Merriman 1999).

1.1.2. *Methods allowing numerical diffusion at the interfaces*

Usually numerical diffusion is considered as a drawback for numerical scheme. But it is a necessary feature for capturing discontinuities. It renders easy the computation of shock or contact discontinuities in gas dynamics applications and it also predicts shock and contact discontinuity formation. In the context of flows with interfaces, we look at a numerical scheme that possesses a similar simplicity: a scheme that works on a fixed grid, that allows interface deformations as large as possible, that deals with inflow and outflow boundary conditions in a simple way, that uses the same numerical scheme for all computational cells (multiphase mixtures, shocks, interfaces, rarefaction waves) and that also predict interface formation. These last features are the most important. Simplicity is a result of the scheme and model generality. Interface formation is a very important feature in cavitation flow modelling. Of course, numerical diffusion is still a drawback, but there are several ways to reduce its effects

https://doi.org/10.1017/S0022112000003098 Published online by Cambridge University Press

as done conventionally in gas dynamics applications: mesh refinement, high-order differencing and other strategies.

(*a*) *Methods based on the Euler equations*

The first efficient method was proposed by Karni (1996). This method was based on the level set technique to locate the interface, and a primitive variable formulation of the Euler equations was used to determine the pressure at the interface. This method, although non-conservative, has proven efficiency for the computation of interface properties between ideal gases. But the extension of this method to reacting flows and real materials was not obvious. Simultaneously, Abgrall (1996) proposed another method for ideal gases in one space dimension. A variant of this method was extended by Shyue (1998) to materials governed by the stiffened gas equation of state and independently by Saurel & Abgrall (1999*b*) again to materials governed by the same equation of state in several space dimensions. This last method can be extended to reacting flows and more general equations of state (Saurel & Mencacci 1999). It has been improved and extended to unstructured grids by Abgrall, Nkonga & Saurel (2000).

All these methods are very efficient and simple to code for relatively simple physical models. Their main disadvantage lies in the conservation errors regarding the partial mass of the various fluids yielding inaccurate internal energies and temperatures at the interface. They are also difficult to extend to arbitrary equations of state. This is one of the reasons why we have developed a method based on a formulation more suitable than the Euler equations. We now review this method.

(*b*) *Methods based on multiphase flows equations*

We have recently proposed a method based on the compressible multiphase flow equations for the computation of interface variables (Saurel & Abgrall 1999*a*). This method is based on a model involving seven equations (when two fluids only are considered). It is able to deal with very general equations of state, and is conservative for the mixture. It provides accurate internal energies and temperatures at the interface. To our knowledge, the Fedkiw and the multiphase methods are the only ones able to do this. Recently, we have proposed a reduced form of the multiphase model (Massoni *et al.* 2000) that possesses this feature.

The success of the multiphase method relies on several key points:

it uses an unconditionally hyperbolic model for two-phase compressible mixtures;

resolution is based on a modified Godunov (1959) scheme involving accurate differencing of the non-conservative terms and equations;

resolution also uses a relaxation procedure to restore pressure and velocity interface conditions based on infinite relaxation parameters.

But the most important feature is that this method does not work only for interface problems. The model takes basic ideas from one proposed by Baer & Nunziato (1986) for the computation of detonation waves in granular materials. We have revisited this model and proposed introducing some slight modifications regarding closure relations and major modifications regarding relaxation parameters. But this model keeps its generality. It is able to model non-equilibrium two-phase flows as well as flows with interfaces. This has important implications for the modelling of shock waves in compressible mixtures, detonation waves in heterogeneous materials, and any flows involving compressible mixtures. It also possesses a very important feature: the method is able to dynamically create interfaces. This may be very important for the simulation of cavitating flows. So this method is able to deal with a wide range of applications as we detail in the next sections.

https://doi.org/10.1017/S0022112000003098 Published online by Cambridge University Press

1.2. *The modelling of detonation waves in solid energetic materials*

These remarks concern the modelling of detonation waves in solid energetic material and do not apply to gaseous detonations. In gaseous detonations, there is no phase change but only a change in chemical composition of the mixture. Also, the molecular collisions are so intense that the assumption of temperature equilibrium between the various components is valid. For detonations in solid explosives this no longer holds. Indeed the detonation is composed of a shock wave propagating in the solid material and followed by a reaction zone where energy is liberated with a finite rate. During the energy liberation the reactive solid material transforms to product gases. When the reaction ends, the flow is a pure gas mixture. But the reaction zone always corresponds to a multiphase mixture. In this multiphase mixture, the assumption of thermal equilibrium is totally wrong: the solid phase has a very different temperature from the burnt gases.

For many applications, the details of the reaction zone has no importance because this zone is very sharp (a few micrometres), and the detonation can be considered as a discontinuity connecting a pure unreacted solid to a mixture of reacted gases. But there are a lot of applications for which the details of this reaction zone are important. For example, with non-ideal explosives, this reaction zone can be of the order of 1 cm to 1 m.

In spite of the above discussion, the modelling in nearly all detonation codes is based on the Euler equations. Since the Euler equations allow determination only of the mixture variables (density, velocity and internal energy) it is necessary to have an equation of state for the mixture in order to compute the pressure. So the difficulty is transferred to the mixture equation of state. To construct a mixture equation of state, it is necessary to know the equations of state for each pure material (for example gas and solid) and two thermodynamic assumptions to couple them. The first thermodynamic assumption that is always used is pressure equilibrium between each phase. This assumption can easily be justified for the problems under study. All the difficulties come from the second equilibrium relation. Most mixture equations of state use the assumption of temperature equilibrium between phases, or density equilibrium, or other equalities between thermodynamic functions. The density equilibrium assumption is of course wrong: there is no reason why the gas and the solid should have the same density. The temperature equilibrium assumption is also wrong: the gas phase during combustion reaches 3000–7000 K while the solid phase after the shock front does not exceed 1000 K.

Thus, we can conclude that constructing a mixture equation of state is not easy and can be inaccurate because there is a lack of thermodynamic information regarding the mixture (only mixture energy and density are known with conventional models).

A way to circumvent this problem is to determine more thermodynamic variables for the multiphase mixture. The consequence is to replace the Euler equations by a multiphase model. In this context, each phase will be governed by its own set of partial differential equation, closed by the equation of state (EOS) of the corresponding pure material. The flow model is then no longer dependent on the mixture EOS model. We will show in the following that the multiphase model used for interface computation can be extended easily to the computation of detonation waves. It just needs some extentions regarding mass and energy transfers. Generality of the model will render easy the computation of the interaction of detonation waves with other materials separated by interfaces. This will be done with the same model and method.

https://doi.org/10.1017/S0022112000003098 Published online by Cambridge University Press

1.3. *The modelling of cavitating flows*

Cavitation occurs in liquids and solids when a pressure drop is such that the resulting thermodynamic state corresponds to a point lying inside the saturation curve. Such a situation may occur when a strong rarefaction wave propagates into a liquid or when acceleration or inertial effects induce a pressure drop.

Cavitation is difficult to model because starting from a pure phase, another phase appears and creates interfaces. To our knowledge, the modelling of cavitating flows has been achieved in specific situations only:

homogeneous bubbly flows;
a single or limited number of interfaces (cavitation pockets);
homogeneous cavitation with mixture models.

(*a*) *Bubbly flows*

There are a lot of models used to study bubbly flows and cavitation phenomena. They are usually based on a continuous model for the mean flow, compressible or not, with a microscopic model for the bubble dynamics based on the Rayleigh equation. The drawbacks of this type of model are that the gas phase must be present initially and that the flow topology is fixed: a bubbly flow only. For instance, cavitation pockets cannot be predicted by this type of model. Examples of these models are given in van Wijngaarden (1972), Tan & Bankoff (1984) and Mazel *et al.* (1996).

(*b*) *Cavitation pockets*

The literature contains many simulations of cavitation pockets around airfoils. These simulations use an iterative method based on incompressible Euler or Navier–Stokes equations in a geometry that evolves during the iterative process. The interface is solved as a slip boundary condition and its position is varied with time in order that the saturation pressure in the gas phase (or local pressure if compressible equations are solved in the gas) be equal to the local liquid pressure. This procedure is of course expensive in computer resources, limited to a small number of interfaces and to steady or quasi-steady conditions.

Another procedure, more suitable for dynamic simulations is based on the VOF method (Hirt & Nichols 1981) and incompressible flow equations. In these methods the interface needs to be settled initially: interface creation is not allowed. Also, the external flow must be single phase: bubbly flows for example are not allowed. Another restriction is related to the incompressible flow assumption. This means that these simulations are restricted to low flow velocities and to weak thermodynamic and kinematic variations inside the gas pocket. Some example of these procedures may be found in Molin *et al.* (1997) and de Jouëtte *et al.* (1997).

(*c*) *Mixture models*

In these models, the flow is modelled with the compressible Euler or Navier–Stokes equations closed by an equation of state valid for all fluid states: pure liquid, pure vapour and a two-phase mixture. The mixture equation of state is based on the phase diagram and assumes pressure and temperature equilibrium. Here, liquid and gas compressibilities are considered, and the assumption of pressure and temperature equilibrium is not as restrictive as in the modelling of detonation waves, because it corresponds to the correct equilibrium conditions inside the saturation region.

Compared to the previous modelling methods, this approach is more suitable for high-velocity flows. Some examples are given in Liou & Edwards (1999) and Saurel, Cocchi & Butler (1999) for highly compressible flow conditions. Unlike the previous modelling, this approach allows interface creation and is fully dynamic. There are

https://doi.org/10.1017/S0022112000003098 Published online by Cambridge University Press

several limitations to this approach. The assumption of thermodynamic equilibrium forbids the study of supercritical states. Also, mass transfer is assumed instantaneous. This means that the flow characteristic times are several orders of magnitude larger than the mass transfer time. This is not always correct. Another important limitation is related to the flow topology. This approach is suitable for cavitation pockets only, or flows where the gas phase is well separated from the liquid phase, whereas cavitation pockets followed by a bubbly flow is a forbidden flow situation. The last limitation is that the mixture equation of state is valid only for flows where the liquid and its vapour only are present. If an uncondensable gas (air in water for example) is present in the flow, the mixture equation of state no longer holds. In many practical situations, the liquid is not a pure fluid and some uncondensable gases are present. They strongly influence the mixture compressibility (bubbles expand before reaching the saturation pressure) and modify the mass transfer dynamics.

(*d*) *Multiphase model*

It is now clear that the previous cavitation models are restricted to specific applications. The multiphase model we propose for interfaces and detonation waves can also be used for cavitation problems. Of course, it cannot cover all the range of interest in cavitation problems, but it possesses several features that render it more general. In particular, it is able to consider compressibility of all phases, takes into account uncondensable gases, is able to model metastable mixtures, creates interfaces dynamically, and also, at least in theory, is able to consider coexisting bubbly flows and cavitation pockets. More generally, this model is able to solve multiphase flows (bubbles, drops, annular flows etc.) and flows with interfaces with the same basic equations, and with the same numerical method. We now detail its main features.

2. The multiphase model

To obtain the multiphase flow model we use the averaging method of Drew & Passman (1998) applied to the compressible Navier–Stokes equations of the various constituents. We then neglect all dissipative terms everywhere except at the interfaces. This model is developed in Saurel & Abgrall (1999*a*) for a two-phase system. It is inspired by the remarkable work of Baer & Nunziato (1986) where a two-phase model is proposed to study the deflagration-to-detonation transition in solid energetic materials. The main difference between Baer & Nunziato's work and the present is related to the use of the relaxation terms. We introduce here the notion of infinite relaxation parameters and instantaneous pressure and velocity equilibrium. This renders possible the numerical treatment of interface problems, and opens the model to a wider range of applications (interfaces, detonations, cavitation, and other multiphase systems). The model is composed of a set of five partial differential equations for each phase k:

$$\frac{\partial \alpha_k}{\partial t} + u_i \nabla \alpha_k = \mu(P_k - P'_k) + m_k/\rho_X, \tag{1}$$

$$\frac{\partial \alpha_k \rho_k}{\partial t} + \nabla(\alpha_k \rho_k u_k) = m_k, \tag{2}$$

$$\frac{\partial \alpha_k \rho_k u_k}{\partial t} + \nabla(\alpha_k \rho_k u_k \otimes u_k + \alpha_k P_k) = P_i \nabla \alpha_k + m_k u_i + F_{dk}, \tag{3}$$

https://doi.org/10.1017/S0022112000003098 Published online by Cambridge University Press

$$\frac{\partial \alpha_k \rho_k E_k}{\partial t} + \nabla(u_k(\alpha_k \rho_k E_k + \alpha_k P_k))$$

$$= P_i u_i \nabla \alpha_k + m_k E_{ki} + F_{dk} u_i + Q_{ki} - \mu P_i (P_k - P'_k), \tag{4}$$

$$\frac{\partial N_k}{\partial t} + \nabla(N_k u_k) = \dot{N}_k, \tag{5}$$

with the average interface conditions:

$$\sum_k m_k = 0, \tag{6}$$

$$\sum_k P_i \nabla \alpha_k + m_k u_i + F_{dk} = 0, \tag{7}$$

$$\sum_k P_i u_i \nabla \alpha_k + m_k E_{ki} + F_{dk} u_i + Q_{ki} - \mu P_i (P_k - P'_k) = 0. \tag{8}$$

The notation is conventional. The volume fraction α_k is defined by the volume occupied by phase k over the total volume. The saturation constraint imposes $\sum \alpha_k = 1$. The density, velocity, pressure and total energy are represented respectively by ρ, u, P and $E = e + 1/2uu$. The subscripts k and i are related to phase k and interface-averaged variables respectively.

The left-hand side of equations (2), (3) and (4) are conventional. On the right-hand side appear the terms related to mass transfer m_k, drag force F_{dk}, heat transfer Q_i and the non-conservative terms $P_i \nabla \alpha_k$ and $P_i u_i \nabla \alpha_k$. The $\mu(P_k - P'_k)$ and $\mu P_i(P_k - P'_k)$ terms are related to the pressure relaxation process. They are of major importance.

Equation (1) expresses the evolution of the phase volume fractions. It comes from the average of a test function equal to 1 in phase k and 0 elsewhere. This equation is a simplification of a more general volume fraction evolution equation accounting for inertial effects (bubble pulsation for example) and other interface kinematics considerations. The generalization of the present model to micro-inertia considerations (bubble pulsation) is given in Gavrilyuk & Saurel (2000). Here, for mathematical, numerical and physical reasons we close the model with this simplified equation.

Equation (5) represents the evolution of the number density of the individual entity composing phase k. For instance, if phase k is the gas phase filling bubbles, N_k then represents the number density of bubbles per unit volume. Knowledge of the number density of individual particles is important for determining the surface of mass, momentum and energy exchanges between phases. The term $\dot{N}_k$ models breakup or coalescence of individual particles.

When the assumption of spherical elemental particles is not valid, the exchange surface determination is a more acute problem. Such a difficulty occurs when the flow changes topology. Determination of the interfacial area in the general case is still an open problem. The interested reader will find information in Drew & Passman (1998) and Morel, Goreaud & Delhaye (1999).

Before giving details about the various terms, let us give a simple picture of the physical meaning of the non-conservative terms $P_i \nabla \alpha_k$ and $P_i u_i \nabla \alpha_k$. The one-dimensional Euler equations averaged over a duct of variable cross-section A, in the absence of mass, momentum and heat transfer are:

$$\frac{\partial A\rho}{\partial t} + \frac{\partial (A\rho u)}{\partial x} = 0, \tag{9}$$

https://doi.org/10.1017/S0022112000003098 Published online by Cambridge University Press

$$\frac{\partial A\rho u}{\partial t} + \frac{\partial A(\rho u^2 + P)}{\partial x} = P\frac{\partial A}{\partial x}, \tag{10}$$

$$\frac{\partial A\rho E}{\partial t} + \frac{\partial Au(\rho E + P)}{\partial x} = -P\frac{\partial A}{\partial t}. \tag{11}$$

In two-phase systems, the volume fraction α is sometimes used as a surface fraction. If we make this analogy, and replace the temporal derivative $\partial A/\partial t$ by a space derivative $u\,\partial A/\partial x$ with the help of equation (1), we recover the same equations for the one-dimensional averaged Euler equations and the multiphase model.

This means that the non-conservative terms in the multiphase model have the same effect as the duct variation cross-section terms: nozzling terms. Their effects are well known in steady flows: acceleration of subsonic flows in area restriction for example. This simple picture can be important for the derivation of numerical schemes, or results analysis.

This also means that the multiphase model, in a certain sense, couples several Euler systems in 'ducts' of variable cross-section. These 'ducts' have permeable walls for the various transfers, are moving with the flow at velocity u_i and expanding with the pressure differential $\mu(P_k - P_k')$ at a rate controlled by μ.

We now give some details about the closure relations.

2.1. *Closure relations independent of the physical processes*

When dealing with two-phase gas–liquid flows at low pressure and velocity, the most natural idea is to consider the liquid phase incompressible. Then, the interfacial pressure is taken equal to the gas pressure. This choice yields an ill-posed mathematical model (see for example Drew & Passman 1998), which results in numerical instabilities during numerical resolution, or in the necessity of using an extremely large numerical viscosity yielding unrealistic solutions.

Other authors (Toro 1989; Sainsaulieu 1995) have proposed introducing a pressure non-equilibrium effect, $P_i(\alpha)$. In Sainsaulieu (1995), P_i is a perturbation term that enables the system to be hyperbolic. In Toro (1989), this term represents compaction effects in a packed powder bed. Other authors (Powers, Stewart & Krier 1990) assume $P_i = 0$. This choice is non-justifiable. It cancels the nozzling effects mentioned previously. However, considering each phase compressible yields a hyperbolic system even if $P_i = 0$.

In our approach, each phase is considered compressible with its own pressure and velocity. This guarantees hyperbolicity. So, there is some freedom in the choice of closure relations for interfacial pressure and velocity with respect to hyperbolicity. But for physical reasons, the interfacial pressure and velocity must be estimated as accurately as possible. Unfortunately, this is nearly impossible in the general case. For the specific context of stratified flows, it is possible to estimate an interfacial pressure on the basis of the velocity and density differences (Bestion 1990). For flow of gases and solid particles under weak solid compressibility, it is reasonable to assume the interfacial pressure to be the gas one, and interfacial velocity to be the solid one (Baer & Nunziato 1986). In fact, for each physical situation, there are choices better than other, but none is perfectly satisfactory.

For the applications we will show here, the velocities and pressures of all phases will be relaxed instantaneously during numerical resolution. So, our strategy is to choose interfacial variables close to the relaxed state (see later sections). Because each phase is compressible, a choice preserving symmetry is also preferable. A reasonable estimate that considers compressibility of each phase and preserves symmetry is to

https://doi.org/10.1017/S0022112000003098 Published online by Cambridge University Press

take the interfacial pressure equal to a mixture total pressure:

$$P_i = \sum \alpha_k (P_k + \rho_k (u_i - u_k)^2). \tag{12}$$

This guess is also motivated by the analysis of the Riemann invariants of the model. The phase pressures P_k are given by appropriate equations of state $P_k = P_k(\rho_k, e_k)$. The second interfacial variable is the average interfacial velocity. In most references, u_i is taken equal to the velocity of the incompressible or the less compressible phase (Butler, Lambeck & Krier 1982, Baer & Nunziato 1986; Saurel, Larini & Loraud 1992; Saurel 1996; and Sainsaulieu 1995). As mentioned previously regarding the interfacial pressure, determination of the average interfacial velocity is a formidable task. Again, in the context of compressible multiphase mixtures, the choice of the interfacial velocity does not affect the mathematical nature of the overall system: it remains hyperbolic. So there is some freedom in this choice. But again, for symmetry reasons, and in order to be consistent with the relaxed velocity (see later sections) we set the velocity of the centre of mass as the estimate for the average interfacial velocity:

$$u_i = \sum \alpha_k \rho_k u_k \Big/ \sum \alpha_k \rho_k. \tag{13}$$

We will give other arguments for these estimates when examining the numerical method.

2.2. *Closure relations dependent on the physical processes*

2.2.1. *Non-conventional interaction terms–infinite relaxation terms*

(*a*) *Pressure terms*

The model contains non-conventional interaction terms regarding the pressure relaxation process: $\mu(P_k - P'_k)$ in the volume fraction evolution equation and $\mu P_i(P_k - P'_k)$ in the energy equation. The first term represents the rate of expansion of the volume fraction α_k in order that pressures tend towards equilibrium. The physical meaning of this term is very simple. If the various phases are not in pressure equilibrium after the passage of a rarefaction or shock wave, the volume of each phase must vary in order that pressure tends to equilibrium. The variable μ controls the rate at which this equilibrium will be reached. Existence of this variable has been shown theoretically following the second law of thermodynamics and the mechanics of irreversible processes (Baer & Nunziato 1986).

When the pressures are in a non-equilibrium state, the elementary particles (bubbles, drops etc.) undergo a three-dimensional microscopic motion making their volume vary in order that pressures tends toward equilibrium. This three-dimensional motion has not been taken into account in the averaged phase velocities and in our guess for the interfacial velocity (13). Our interfacial velocity represents the average translational motion of the mixture, and the microscopic motion is not considered. Introducing a volume variation function of the pressure differential is a way to correct the estimate for the averaged interfacial velocity, and also a way to take information from the microscopic media.

The homogenization variable μ depends on the compressibility of each fluid (and so of their equations of state), on the nature of each fluid, and on the two-phase mixture topology. So, it is a very difficult variable or function to determine. But for most applications, it may be considered as infinite.

We have shown in Saurel & Abgrall (1999*a*) that these terms are crucial for the computation of pressure waves in two-phase mixtures, but also of paramount

https://doi.org/10.1017/S0022112000003098 Published online by Cambridge University Press

importance for restoring the pressure interface condition when solving interfaces separating compressible pure materials solved with the multiphase flows equations. When a pressure wave travels a multiphase mixture, if the elementary particles are sufficiently small compared to the macroscopic control volume and computational cell, then the time required for an acoustic wave to travel across the elementary particle and equilibrate the particle pressure to the external pressure is much smaller than the characteristic time for the propagation of the macroscopic waves. In such cases, the pressure relaxation parameter can be considered infinite. This situation occurs as well as in solid alloys through which shock waves travel and considered as multiphase mixtures, as in detonation waves in solid explosives, as will be detailed later, and of course at interfaces between pure materials. Actually, at the interfaces, instantaneous pressure equality between phases is mandatory.

Note that pressure equilibrium is not the required condition when:

(i) Inertial effects are accounted for in a more sophisticated model than equation (1) (Gavrilyuk & Saurel 2000);

(ii) The materials do not have a fluid behaviour. If material k is a plastic solid for example, the volume fraction evolution term will be $\mu(P_k + P_{Yk}/r - P'_k)$ where P_{Yk} is the elastic limit of material k, and r is the microscopic displacement from the initial equilibrium condition.

(iii) Surface tension effects are considered. In such a case, if material k possesses a surface tension the volume fraction evolution term will be $\mu(P_k + \sigma_k/r - P'_k)$ where σ_k is the surface tension of material k, and r the radius of curvature of the interface of the elementary particle.

(iv) Elementary particles have collisions. For example, when the mixture contains solid packed powder grains the actions of grains over neighbouring grains may be summarized in an intergranular stress tensor (Kuo, Yang & Moore 1980; Toro 1989). Then the volume fraction evolution term is $\mu(P_k + P_{gk}(\alpha_k) - P'_k)$ where $P_{gk}(\alpha_k)$ represents the action due to the surrounding particles under confining conditions.

To summarize, it is necessary to use the difference of normal constraints in equation (1) when the material is not an ideal fluid.

Finally, the term $\mu P_i(P_k - P'_k)$ in the energy equation represents the pressure work during the pressure relaxation process.

(*b*) *Velocity terms*

The velocity relaxation term is the most conventional one in multiphase systems and is represented by the drag force F_{dk}. What is not conventional in our approach is to consider an infinite relaxation drag coefficient for the applications under interest.

Let us first recall briefly what the drag force F_{dk} represents. With a multiphase flow model, details of the flow microstructure are not available because only averaged quantities are determined. The drag force over an elementary particle (bubble, drop) corresponds to the sum of constraints induced by the various materials, at the interface. There is a part due to viscous or deviatoric constraints (viscous drag force) and a part due to the spherical part of the strain tensor (pressure drag force). Inside a multiphase control volume, expressions for these forces need knowledge of the microscopic flow structure, which is of course not available. So, in general, drag force is introduced as an empirical relation coming from experiments, or from a submodel. Conventional drag correlations are a function of the local Reynolds number. Here we give an example with a correlation from Rowe (1961) for a dilute two-phase solid–gas mixture:

$$F_d = 6\pi R\mu_g(u_s - u_g)N_sC_d \tag{14}$$

https://doi.org/10.1017/S0022112000003098 Published online by Cambridge University Press

with the drag coefficient defined by $C_d = 1 + 0.15Re^{0.687}$ if $Re < 1000$ and $C_d = 0.01833Re$ otherwise. The particles are assumed spherical, and their radius R is obtained from the relation between volume fraction and number density of particles: $\alpha_s = 1 - \alpha_g = N_s \frac{4}{3}\pi R^3$. The Reynolds number is expressed as $Re = 2R\rho_g|u_s - u_g|/\mu_g$.

The general drag force may be written in the form

$$F_{dk} = \lambda_k(u_k - u'_k) \tag{15}$$

where λ_k is a positive finite function (or vector if there are more than two fluids). It controls the rate at which velocities tend towards equilibrium. In special physical situations, this function tends to infinity, for example in materials with a very high deviatoric stress tensor (gas pores inside a solid). Such a situation has been studied recently by Kapila *et al.* (1997) in the limit of very high drag coefficients.

On the other hand, for reasons related to the numerical method when solving interface problems between pure fluids with the multiphase model, we have shown that missing characteristic directions at the interface may be replaced by source terms with infinite pressure and velocity relaxation coefficients (Saurel & Abgrall 1999*a*). We have explained in the previous section that the first interface condition could be restored with an infinite μ coefficient. To restore the second interface condition (velocity equality), an infinite drag coefficient λ must be used. The numerical procedure with infinite relaxation coefficients will be detailed in a subsequent section for an arbitrary number of fluids.

2.2.2. *Conventional interaction terms–finite relaxation terms*

(*a*) *Mass and energy transfers*

The mass transfer term m_k is usually given by empirical relations depending on the process under study: evaporation, condensation, combustion etc. For example, to model the combustion of solid propellant particles in a gas, the simplest model available is based on Vieille's law. It expresses the rate of particle size regression as a function of pressure: $\mathrm{d}R/\mathrm{d}t = aP_g^n$ where a and n are empirical constants. Then, the mass transfer is

$$m_s = \rho_s S_s N_s \frac{\mathrm{d}R}{\mathrm{d}t} \tag{16}$$

where the subscript s denotes solid particles. S_s represents the surface of an individual particle ($S_s = 4\pi R^2$).

For specific applications, more detailed models are preferred to Vieille's law. When a detailed description of propellant combustion is necessary, models based on the flame structure may be used (Mitani & Williams 1986). A mechanistic model based on pore collapse mechanics is developed in Massoni *et al.* (1999) for the dynamics of shock-to-detonation transition in solid energetic materials. In other mass transfer problems (evaporation, condensation, cavitation), without chemical transformation, the mass transfer reduces to a phase change problem and is obtained from the interface-averaged equations.

Substitution of the mass (6) and the momentum (7) interface equation in the interface energy equation (8) yields in the simplified case of a two-phase system

$$m_1 = -(Q_{1i} + Q_{2i})/(E_{1i} - E_{2i}). \tag{17}$$

This relation shows that the mass transfer is a function of the heat transfer. Heat transfers are usually provided by empirical correlations based on the Nusselt number:

$$Q_{ki} = h_k(T_{ki} - T_k)A_{ex} \tag{18}$$

https://doi.org/10.1017/S0022112000003098 Published online by Cambridge University Press

where h_k represents the heat exchange coefficient, T_{ki} the interface temperature, T_k temperature of phase k and A_{ex} the exchange area between phase k and the interface. For evaporating liquid droplets in a gas flow, Yuen & Chen (1977) have proposed an empirical correlation for the Nusselt number:

$$Nu = 2 + 0.6Re^{0.5}Pr^{0.33} \tag{19}$$

where Re represents the Reynolds number defined previously and Pr the Prandtl number. This correlation provides an easy expression for the heat exchange coefficient:

$$h_g = \lambda_g Nu/(2R) \tag{20}$$

where λ_g is the gas conductivity.

In such two-phase flows where the topology and geometry of elemental particles is estimated with a reasonable accuracy by spherical particles, the exchange interfacial area is simply $A_{ex} = N_l S_l$ where $S_l = 4\pi R^2$ represents the surface of an individual droplet.

When mass transfer occurs, an extra source term is present in equation (1) and involves a density ρ_X. This density must be chosen equal to that of the less compressible material. The reason is that mass transfer phenomena induce acoustic waves. Thus, the pressure relaxation process is coupled to the mass transfer. Since it is very difficult to solve these two phenomena in a fully coupled way, we separate the acoustic propagation and the mass transfer during numerical resolution. Thus, within a time step, the best estimates for the volume changes due to mass transfer are the ones based on the less compressible material. The partial volumes are then adjusted by the pressure relaxation procedure.

(*b*) *Breakup and coalescence*

Breakup and coalescence phenomena are related to the interfacial area determination. Coalescence modelling is a very difficult task and can be achieved in only limited situations. Breakup phenomena are usually modelled on the basis of hydrodynamic instabilities and are also limited to simplified situations: bubbly and droplet flows. An empirical model based on Weber number for droplet breakup may be found in Kolev (1993). When the flow consists in gas–droplets only, breakup modelling consists of determining the source term of equation (5): $\dot{N}_k$. Application of the Kolev breakup mechanism in two-phase flow modelling is given in Utheza *et al.* (1996).

3. Numerical method

For all applications previously mentioned we have to solve an hyperbolic system, involving non-conservative terms and equations, and finite and infinite relaxation terms. Unconditional hyperbolicity has been demonstrated in Saurel & Abgrall (1999*a*). It can also be easily shown that the summation of other all phases of the mass, momentum and energy equations reduces to the mixture Euler equations. So the mixture is perfectly conservative. Frame invariance of the equations can also be easily demonstrated.

When a first-order numerical scheme is employed, we need three types of integrators to reach the solution, provided that the Strang splitting is assumed valid. The solution is obtained by a succession of operators (Strang 1968):

$$U_i^{n+1} = L_S^{\Delta t} L_R^{\Delta t} L_H^{\Delta t} U_i^n. \tag{21}$$

L_S represents the integration operator for source terms: mass and energy finite rate transfers. When velocity and pressure relaxation are also finite rate, L_S is used instead

https://doi.org/10.1017/S0022112000003098 Published online by Cambridge University Press

of L_R, the infinite relaxation operator. We do not provide details of the L_S operator. It is a standard ODE solver, and its accuracy and robustness are dependent on the problem stiffness (for example see Byrne & Dean 1992).

An expression for the infinite relaxation operator L_R is not easy to obtain. We have provided a detailed description of it in Saurel & Abgrall (1999*a*) in the context of two fluids only. We generalize it in the following for an arbitrary number of materials, governed by arbitrary equations of state. This is of major importance for the applications with detonations and hydrocodes, where a large number of materials coexist. But the major difficulties lie in the hyperbolic solver L_H which we now describe. Basic elements are again given in Saurel & Abgrall (1999*a*). We generalize it here to the multidimensional case after recalling the basic ideas.

3.1. *Hyperbolic operator*

The numerical method we are developing applies at all mesh points: single phase, two phase and at the interfaces. For the sake of simplicity and generality regarding complex equations of state for the various fluids, we have retained the simplest ingredients for the construction of a high-resolution scheme for two-phase flows with arbitrary equations of state. The Riemann solver is chosen for an easy implementation with the various models and equations of state, even though its accuracy could be improved.

The hyperbolic system involves several difficulties. Non-conservative terms and a non-conservative equation (the volume fraction evolution equation) are present. We have proposed in Saurel & Abgrall (1999*a*) an efficient way to discretize these terms. The main idea that guides the building of the numerical scheme can be stated as follows:

If a multiphase flow evolves under uniform pressure and velocity conditions, it must remain uniform under the same variables during time evolution.

This has been systematically exploited in the context of the Euler equations and has shown that it provided an efficient discretization scheme for non-conservative equations even when velocity and pressure were not initially uniform (Saurel & Abgrall 1999*b*).

3.1.1. *One-dimensional first-order method*

For the sake of simplicity we first explain the method in one dimension with a first-order Godunov type scheme. We then generalize it in multidimensions and second order. The equations to solve for each phase k are

$$\left.\begin{aligned} &\frac{\partial \alpha_k}{\partial t} + u_i \frac{\partial \alpha_k}{\partial x} = 0, \\ &\frac{\partial \boldsymbol{U}}{\partial t} + \frac{\partial F(\boldsymbol{U})}{\partial x} = H(\boldsymbol{U}) \frac{\partial \alpha_k}{\partial x}, \end{aligned}\right\} \tag{22}$$

with $\boldsymbol{U} = (\alpha_k\rho_k, \alpha_k\rho_k u_k, \alpha_k\rho_k E_k, N_k)^T$, $F(\boldsymbol{U}) = (\alpha_k\rho_k u_k, \alpha_k\rho_k u_k^2 + \alpha_k P_k, u_k(\alpha_k\rho_k E_k + \alpha_k P_k), N_k u_k)^T$, and $H(\boldsymbol{U}) = (0, P_i, P_i u_i, 0)$.

In quasi-linear form with primitive variables, this system is

$$\frac{\partial \boldsymbol{W}}{\partial t} + A(\boldsymbol{W}) \frac{\partial \boldsymbol{W}}{\partial x} = 0 \tag{23}$$

https://doi.org/10.1017/S0022112000003098 Published online by Cambridge University Press

with $\boldsymbol{W} = (\alpha_k, \rho_k, u_k, P_k, N_k)^T$ and

$$\boldsymbol{A}(\boldsymbol{W}) = \begin{pmatrix} u_i & 0 & 0 & 0 & 0 \\ \rho_k/\alpha_k(u_k - u_i) & u_k & \rho_k & 0 & 0 \\ (P_k - P_i)/\alpha_k\rho_k & 0 & u_k & 1/\rho_k & 0 \\ \rho_k c_{ki}^2/\alpha_k(u_k - u_i) & 0 & \rho_k c_k^2 & u_k & 0 \\ 0 & 0 & N_k & 0 & u_k \end{pmatrix}.$$

The Jacobian matrix $\boldsymbol{A}(\boldsymbol{W})$ admits the following eigenvalues: $u_i, u_k + c_k, u_k - c_k$ and u_k. So the system is hyperbolic. Note that the Euler system eigenvalues are recovered, augmented by an extra one which is u_i.

Knowledge of these wave speeds is necessary for the Riemann solver. For the numerical approximation of the conservative fluxes $F(\boldsymbol{U})$ we use the HLL (Harten, Lax & van Leer 1983) Riemann solver. At a cell boundary separating right (R) and left (L) states, the corresponding flux is

$$F^* = (S_R F_L - S_L F_R + S_R S_L (U_R - U_L))/(S_R - S_L) \tag{24}$$

where the waves speed S_R and S_L are estimated by

$$S_R = \mathrm{Max}_k\,(0, (u_k + c_k)_R, (u_k + c_k)_L) \quad \text{and} \quad S_L = \mathrm{Min}_k\,(0, (u_k - c_k)_R, (u_k - c_k)_L)$$

It is now necessary to determine the discretization formulas for the non-conservative terms and equation. To obtain these formulas, we develop over a time step the Godunov scheme with the HLL flux for each equation. We then pose that the pressure and velocities are uniform. Under the restriction that the flow must retain the same pressure and velocity, we will find the corresponding formulas for the non-conservative terms and equation.

The Godunov scheme with HLL flux for the quasi-conservative system (second equation of system (22)) is

$$U_i^{n+1} = U_i^n - \lambda(F^*_{i+1/2} - F^*_{i-1/2}) + H(U_i^n)\Delta \tag{25}$$

where $\lambda = \Delta t/\Delta x$ and Δ represents the numerical approximation of $\partial\alpha_k/\partial x$ which we now give.

We start from the mass conservation equation of phase k:

$$(\alpha_k\rho_k)_i^{n+1} = (\alpha_k\rho_k)_i^n - \lambda(\Omega_{i+1/2} - \Omega_{i-1/2})$$

with

$$\Omega_{i+1/2} = \frac{S^R_{i+1/2}(\alpha_k\rho_k u_k)_i^n - S^L_{i+1/2}(\alpha_k\rho_k u_k)_{i+1}^n + S^R_{i+1/2}S^L_{i+1/2}((\alpha_k\rho_k)_{i+1}^n - (\alpha_k\rho_k)_i^n)}{S^R_{i+1/2} - S^L_{i+1/2}}.$$

Assuming $u^n_{k_{i-1}} = u^n_{k_i} = u^n_{k_{i+1}} = u$ we obtain

$$\Omega_{i+1/2} = \frac{u(S^R_{i+1/2}(\alpha_k\rho_k)_i^n - S^L_{i+1/2}(\alpha_k\rho_k)_{i+1}^n) + S^R_{i+1/2}S^L_{i+1/2}((\alpha_k\rho_k)_{i+1}^n - (\alpha_k\rho_k)_i^n)}{S^R_{i+1/2} - S^L_{i+1/2}}.$$

We now consider the momentum equation. Assuming pressure uniformity $P^n_{k_{i-1}} = P^n_{k_i} = P^n_{k_{i+1}} = P$ we obtain

$$(\alpha_k\rho_k u_k)_i^{n+1} = (\alpha_k\rho_k u_k)_i^n - \lambda(\Psi_{i+1/2} - \Psi_{i-1/2}) + \Delta t P \Delta$$

https://doi.org/10.1017/S0022112000003098 Published online by Cambridge University Press

where

$$\Psi_{i+1/2} = u\frac{u(S^R_{i+1/2}(\alpha_k\rho_k)^n_i - S^L_{i+1/2}(\alpha_k\rho_k)^n_{i+1}) + S^R_{i+1/2}S^L_{i+1/2}((\alpha_k\rho_k)^n_{i+1} - (\alpha_k\rho_k)^n_i)}{S^R_{i+1/2} - S^L_{i+1/2}}$$
$$+P\frac{S^R_{i+1/2}(\alpha_k)^n_i - S^L_{i+1/2}(\alpha_k)^n_{i+1})}{S^R_{i+1/2} - S^L_{i+1/2}}.$$

From the mass and momentum equations, it is clear that in order that the velocity at time t_{n+1} be equal to that at time t_n it is necessary that the non-conservative term be discretized by

$$\Delta = \frac{1}{\Delta x}\left(\frac{S^R_{i+1/2}(\alpha_k)^n_i - S^L_{i+1/2}(\alpha_k)^n_{i+1}}{S^R_{i+1/2} - S^L_{i+1/2}} - \frac{S^R_{i-1/2}(\alpha_k)^n_{i-1} - S^L_{i-1/2}(\alpha_k)^n_i}{S^R_{i-1/2} - S^L_{i-1/2}}\right). \tag{26}$$

So, the numerical approximation of $\partial\alpha_k/\partial x$ is determined.

We now consider the energy equation under uniform pressure and velocity conditions. After some simplifications we obtain

$$(\alpha_k\rho_k e_k)^{n+1}_i = (\alpha_k\rho_k e_k)^n_i - \lambda(\Phi_{i+1/2} - \Phi_{i+1/2})$$

where

$$\Phi_{i+1/2} = \frac{u(S^R_{i+1/2}(\alpha_k\rho_k e_k)^n_i - S^L_{i+1/2}(\alpha_k\rho_k e_k)^n_{i+1}) + S^R_{i+1/2}S^L_{i+1/2}((\alpha_k\rho_k e_k)^n_{i+1} - (\alpha_k\rho_k e_k)^n_i)}{S^R_{i+1/2} - S^L_{i+1/2}}.$$

We now introduce the equation of state. An equation of state valid for gases, liquids and solids under hydrodynamic regime is the stiffened gas equation of state: $\rho_k e_k = (P_k + \gamma_k P_{inf_k})/(\gamma_k - 1)$. Since γ_k and P_{inf_k} are constant parameters of phase k and pressure P_k is uniform, each product $\rho_k e_k$ is constant. This yields

$$\alpha^{n+1}_{k_i} = \alpha^n_{k_i} - \lambda\left(u\left(\frac{S^R_{i+1/2}\alpha^n_{k_i} - S^L_{i+1/2}\alpha^n_{k_{i+1}}}{S^R_{i+1/2} - S^L_{i+1/2}} - \frac{S^R_{i-1/2}\alpha^n_{k_{i-1}} - S^L_{i-1/2}\alpha^n_{k_i}}{S^R_{i-1/2} - S^L_{i-1/2}}\right)\right.$$
$$\left. + \frac{S^R_{i+1/2}S^L_{i+1/2}(\alpha^n_{k_{i+1}} - \alpha^n_{k_i})}{S^R_{i+1/2} - S^L_{i+1/2}} - \frac{S^R_{i-1/2}S^L_{i-1/2}(\alpha^n_{k_i} - \alpha^n_{k_{i-1}})}{S^R_{i-1/2} - S^L_{i-1/2}}\right). \tag{27}$$

This equation is simply a numerical approximation of $\partial\alpha_k/\partial t + u\partial\alpha_k/\partial x = 0$. The factor of u is again the discretization of $\partial\alpha_k/\partial x$, and the other term is a viscous one.

It is important to note that the discretization of the non-conservative terms is strongly dependent on the Riemann solver, and discretization of the non-conservative equation makes a viscous term appear that is also dependent on the solver.

The last equation, expressing the conservation of the number density of elementary particles, is uncoupled from the overall system and is solved without difficulty with scheme (25). To summarise, system (22) is solved by the following method:

the first equation of system (22) is solved by (27);

the other part of system (22) is solved by (25), with numerical flux (24) and numerical approximation of non-conservative term (26).

This scheme is stable under the standard CFL condition, based on the largest absolute wave speed.

This method can be extended to second order and multidimensions and details are provided next.

https://doi.org/10.1017/S0022112000003098 Published online by Cambridge University Press

3.1.2. *Two-dimensional second-order method*

The system to solve now is:

$$\left.\begin{aligned} \frac{\partial \alpha_k}{\partial t} + u_i \frac{\partial \alpha_k}{\partial x} + v_i \frac{\partial \alpha_k}{\partial y} &= 0, \\ \frac{\partial \boldsymbol{U}}{\partial t} + \frac{\partial F(\boldsymbol{U})}{\partial x} + \frac{\partial G(\boldsymbol{U})}{\partial y} &= H(\boldsymbol{U}) \frac{\partial \alpha_k}{\partial x} + I(\boldsymbol{U}) \frac{\partial \alpha_k}{\partial y}, \end{aligned}\right\} \tag{28}$$

with

$$\boldsymbol{U} = (\alpha_k \rho_k, \alpha_k \rho_k u_k, \alpha_k \rho_k v_k, \alpha_k \rho_k E_k, N_k)^T,$$

$$\boldsymbol{F}(\boldsymbol{U}) = (\alpha_k \rho_k u_k, \alpha_k \rho_k u_k^2 + \alpha_k P_k, \alpha_k \rho_k u_k v_k, u_k(\alpha_k \rho_k E_k + \alpha_k P_k), N_k u_k)^T,$$

$$\boldsymbol{G}(\boldsymbol{U}) = (\alpha_k \rho_k v_k, \alpha_k \rho_k u_k v_k + \alpha_k \rho_k v_k^2 + \alpha_k P_k, v_k(\alpha_k \rho_k E_k + \alpha_k P_k), N_k v_k)^T,$$

$$\boldsymbol{H}(\boldsymbol{U}) = (0, P_i, 0, P_i u_i, 0) \text{ and } \boldsymbol{I}(\boldsymbol{U}) = (0, 0, P_i, P_i v_i, 0).$$

The basic ingredients of the finite volume method used here are described in Toro (1997) in the context of the Euler equations. We consider a computational cell i in the two-dimensional (x, y) space. Note that n_{ij} is the external unit normal vector of the j side of cell i: $n_{ij} = (n_{ijx}, n_{ijy})^T$. Also, $\boldsymbol{K} = (\boldsymbol{F}, \boldsymbol{G})$ is the tensor of fluxes and $\boldsymbol{S} = (\boldsymbol{H}, \boldsymbol{I})$ the non-conservative vectors.

As done previously with the Godunov scheme, we first have to consider the second equation of system (28): $\partial \boldsymbol{U}/\partial t + \nabla \cdot \boldsymbol{K} = \boldsymbol{S} \cdot \nabla \alpha_k$. Integrating this equation over a fixed control volume V delimited by its sides, yields

$$V \frac{\partial \boldsymbol{U}}{\partial t} + \sum_{sides} \int \boldsymbol{T}^{-1} \boldsymbol{F}(\boldsymbol{T}\boldsymbol{U})\, \mathrm{d}L = \int (\boldsymbol{S} \cdot \nabla \alpha_k)\, \mathrm{d}V$$

where $\boldsymbol{T}$ is the rotation matrix and $\boldsymbol{T}^{-1}$ is its inverse.

A first-order time and space approximation yields the following result:

$$U_i^{n+1} = U_i^n - \Delta t / V_i \sum_{j=1}^{4} T_{ij}^{-1} L_{ij} \widehat{F_{ij}^*} + \Delta t(\boldsymbol{H}(U_i^n)\Delta_x + \boldsymbol{I}(\boldsymbol{U}_i^n)\Delta_y)$$

where Δ_x and Δ_y are numerical approximations of $\partial \alpha_k/\partial x$ and $\partial \alpha_k/\partial y$, L_{ij} is the length of the j side of cell i and $\widehat{F_{ij}^*}$ is the HLL numerical flux on the corresponding cell boundary in the rotated frame of reference (along the normal n_{ij}):

$$\widehat{F_{ij}^*} = (S_{Rj}\widehat{F_{Lj}} - S_{Lj}\widehat{F_{Rj}}) + S_{Rj}S_{Lj}(\widehat{U_{Rj}} - \widehat{U_{Lj}})/(S_{Rj} - S_{Lj})$$

where $\widehat{U_{ij}} = T_{ij}U_{ij}$ and $\widehat{F_{ij}} = F(\widehat{U_{ij}})$. Since $T_{ij}^{-1}\widehat{F_{ij}} = n_{ij}K_{ij}$ the Godunov method is

$$U_i^{n+1} = U_i^n - \lambda \sum_{j=1}^{4} L_{ij}\Phi + \Delta t(H(U_i^n)\Delta_x + I(U_i^n)\Delta_y) \tag{29}$$

with $\Phi = (S_{Rj}n_{ij}K_{Lj} - S_{Lj}n_{ij}K_{Rj}) + S_{Rj}S_{Lj}(U_{Rj} - U_{Lj})/(S_{Rj} - S_{Lj})$ and $\lambda = \Delta t/V_i$.

To determine discretization formulas for the non-conservative terms and equations, we consider a multiphase mixture flowing under uniform pressure and velocity conditions and develop the various steps of the Godunov method (Godunov *et al.* 1979). Then, we assume here that there is no sliding between phases since they are in velocity equilibrium. But there are some situations where it is necessary to

https://doi.org/10.1017/S0022112000003098 Published online by Cambridge University Press

consider sliding effects along a contact discontinuity or an interface. Such situations are explained in Saurel & Abgrall (1999*b*). In that case, the discretization method accounting for sliding effects as detailed in that reference is preferred. Here, we assume that these effects are not of major importance for the practical applications under consideration.

So, under the assumptions $P_k = P_i = P$ and $\boldsymbol{V}_k = \boldsymbol{V}_i = \boldsymbol{V}$ and after the same steps as previously we find

$$\Delta_x = (1/V_i)\sum_{j=1}^{4} L_{ij} n_{ijx} (S_{Rj}\alpha_{k_{Lj}} - S_{Lj}\alpha_{k_{Rj}})/(S_{Rj} - S_{Lj}) \tag{30}$$

and

$$\Delta_y = (1/V_i)\sum_{j=1}^{4} L_{ij} n_{ijy} (S_{Rj}\alpha_{k_{Lj}} - S_{Lj}\alpha_{k_{Rj}})/(S_{Rj} - S_{Lj}) \tag{31}$$

for the numerical approximations of $\partial\alpha_k/\partial x$ and $\partial\alpha_k/\partial y$ respectively.

By doing the same manipulations as previously with the energy equation we find the discretization formula for the volume fraction evolution equation:

$$(\alpha_k)_i^{n+1} = (\alpha_k)_i^n - \lambda \sum_{j=1}^{4} L_{ij}\Omega \tag{32}$$

with $\Omega = (n_{ij} \cdot (\boldsymbol{V})(S_{Rj}\alpha_{k_{Lj}} - S_{Lj}\alpha_{k_{Rj}}) + S_{Rj}S_{Lj}(\alpha_{k_{Rj}} - \alpha_{k_{Lj}}))/(S_{Rj} - S_{Lj})$.

The Godunov method (29), with non-conservative approximations (30) and (31) and non-conservative scheme (32) constitutes the first-order two-dimensional method to use for the numerical resolution of system (28). We now examine its second-order extension. This extension follows MUSCL strategy (van Leer 1979). The predictor step is done under a primitive variables formulation. This choice of variables ensures that pressure and velocity will remain uniform after the predictor step, when starting from uniform conditions.

Predicted variables are computed at the middle of each cell boundary with

$$W_{ij}^{n+1/2} = W_i^n + (x_{cij} - x_i)\delta_x W_i + (y_{cij} - y_i)\delta_y W_i \\ -\Delta t/2(A(W_i^n)\delta_x W_i + B(W_i^n)\delta_y W_i) \tag{33}$$

where (x_{cij}, y_{cij}) and (x_i, y_i) are the cell boundary and control volume centre coordinates respectively, W is the primitive variables vector, $\boldsymbol{A}(\boldsymbol{W})$ and $\boldsymbol{B}(\boldsymbol{W})$ the Jacobian matrices, and $\delta_x W_i$, $\delta_y W_i$ the limited slopes along each direction. The primitive variables vector is $\boldsymbol{W} = (\alpha_k, \rho_k, u_k, v_k, P_k, N_k)^T$ and the Jacobian matrices are:

$$\boldsymbol{A}(\boldsymbol{W}) = \begin{pmatrix} u_i & 0 & 0 & 0 & 0 & 0 \\ \rho_k/\alpha_k(u_k - u_i) & u_k & \rho_k & 0 & 0 & 0 \\ (P_k - P_i)/\alpha_k\rho_k & 0 & u_k & 0 & 1/\rho_k & 0 \\ 0 & 0 & 0 & u_k & 0 & 0 \\ \rho_k c_{ki}^2/\alpha_k(u_k - u_i) & 0 & \rho_k c_k^2 & 0 & u_k & 0 \\ 0 & 0 & N_k & 0 & 0 & u_k \end{pmatrix}$$

https://doi.org/10.1017/S0022112000003098 Published online by Cambridge University Press

$$\boldsymbol{B}(\boldsymbol{W}) = \begin{pmatrix} v_i & 0 & 0 & 0 & 0 & 0 \\ \rho_k/\alpha_k(v_k - v_i) & v_k & 0 & \rho_k & 0 & 0 \\ 0 & 0 & v_k & 0 & 0 & 0 \\ (P_k - P_i)/\alpha_k\rho_k & 0 & 0 & v_k & 1/\rho_k & 0 \\ \rho_k c_{ki}^2/\alpha_k(v_k - v_i) & 0 & 0 & \rho_k c_k^2 & v_k & 0 \\ 0 & 0 & 0 & N_k & 0 & v_k \end{pmatrix}.$$

Then, by developing again the Godunov scheme over a time step, the resulting final scheme is (corrector step):

$$\left.\begin{aligned} (\alpha_k)_i^{n+1} &= (\alpha_k)_i^n - \lambda \sum_{j=1}^{4} L_{ij}\Omega \\ \text{and} \\ U_i^{n+1} &= U_i^n - \Delta t/V_i \sum_{j=1}^{4} T_{ij}^{-1} L_{ij} \widehat{F_{ij}^{*n+1/2}} + \Delta t(H(U_i^{n+1/2})\Delta_x + I(U_i^{n+1/2})\Delta_y) \end{aligned}\right\} \quad (34)$$

with

$$\Omega = \frac{n_{ij} \cdot (\boldsymbol{V}_i)^{n+1/2}(S_{Rj}^{n+1/2}\alpha_{k_{Lj}}^{n+1/2} - S_{Lj}^{n+1/2}\alpha_{k_{Rj}}^{n+1/2}) + S_{Rj}^{n+1/2}S_{Lj}^{n+1/2}(\alpha_{k_{Rj}}^{n+1/2} - \alpha_{k_{Lj}}^{n+1/2})}{S_{Rj}^{n+1/2} - S_{Lj}^{n+1/2}}$$

$$\Delta_x = 1/V_i \sum_{j=1}^{4} L_{ij} n_{ijx}(S_{Rj}^{n+1/2}\alpha_{k_{Lj}}^{n+1/2} - S_{Lj}^{n+1/2}\alpha_{k_{Rj}}^{n+1/2})/(S_{Rj}^{n+1/2} - S_{Lj}^{n+1/2})$$

$$\Delta_y = 1/V_i \sum_{j=1}^{4} L_{ij} n_{ijy}(S_{Rj}^{n+1/2}\alpha_{k_{Lj}}^{n+1/2} - S_{Lj}^{n+1/2}\alpha_{k_{Rj}}^{n+1/2})/(S_{Rj}^{n+1/2} - S_{Lj}^{n+1/2})$$

We now have to examine the various source and relaxation operators in the specific context of infinitely fast relaxation processes.

3.2. *Source and relaxation operators*

The relaxation terms are particularly important since they allow the resolution of the interface conditions. This particular procedure involves infinite relaxation coefficients in order that interface conditions be satisfied at any time. The same procedure is also used for detonation modelling in solid explosives. The characteristic time for a solid grain to be in pressure equilibrium with the gas is of the order of the particle diameter divided by the solid sound speed. This time is always smaller or of the same order as the hydrodynamic time step. So, instantaneous pressure equilibrium is a correct assumption.

Regarding velocity relaxation in the explosive, the same type of remark holds. Initially, the gas is filling pores and after shock wave propagation must move with the velocity of the surrounding material. In this situation the velocity relaxation process can be considered instantaneous. During reaction, the gas volume fraction increases, starting from a state where the velocities are equal. Then the pores dislocate and the

https://doi.org/10.1017/S0022112000003098 Published online by Cambridge University Press

grains and gas are free. But effects related to viscosity and density cannot allow too large velocity differences. Indeed the gas density is very high (of the order $1\,\mathrm{g\,cm^{-3}}$). To conclude, even if velocity differences are possible, their experimental measurement is not possible under detonation conditions. So, the best estimate is to consider an infinite drag coefficient.

Considering now cavitating flow, we consider it as an interface problem with dynamic interface creation and mass transfer. So again, pressure equilibrium and macroscopic velocity equilibrium are needed. The solution of the overall problem has a physical sense only after the relaxation procedure step. So this step is of paramount importance.

As in equation (21), we have to solve source terms (finite rate relaxation) as must done for example with mass transfer, and relaxation terms (infinite rate relaxation) for pressure and velocity. We begin with this last one.

3.2.1. *Velocity relaxation operator*

For each phase k we have to solve the ODE system

$$\left.\begin{aligned} \frac{\partial \alpha_k}{\partial t} &= 0, \\ \frac{\partial \alpha_k \rho_k}{\partial t} &= 0, \\ \frac{\partial \alpha_k \rho_k u_k}{\partial t} &= \lambda(u_{k'} - u_k), \\ \frac{\partial \alpha_k \rho_k E_k}{\partial t} &= \lambda u_i (u_{k'} - u_k), \end{aligned}\right\} \tag{35}$$

where the relaxation coefficient λ tends to infinity. This means that for any arbitrary small time increment, the velocities must be in equilibrium.

Combination of the mass and momentum equations yields

$$\frac{\partial u_k}{\partial t} = \lambda(u_{k'} - u_k)/(\alpha_k \rho_k)$$

for phase k and

$$\frac{\partial u_{k'}}{\partial t} = -\lambda(u_{k'} - u_k)/(\alpha_{k'} \rho_{k'})$$

for phase k'. Substracting the first equation from the second and integrating yields the expected result: $u_k^* - u_{k'}^* = 0$. Then, summing the same equations and integrating yields the relaxed velocity

$$u_k^* = \sum (\alpha_k \rho_k u_k)_0 \Big/ \sum (\alpha_k \rho_k)_0 \tag{36}$$

where the subscript 0 indicates the solution obtained from the hyperbolic solver. Some remarks are in order. This relaxed velocity corresponds to the estimate we have proposed for the averaged interfacial velocity (13). So, in all situations where velocities are relaxed instantaneously, the estimated (13) is an accurate prediction of the relaxed state. Note also that the relaxation procedure is an exact one, and a straightforward extension of the two-fluid case as derived in Saurel & Abgrall (1999).

It now remains to update the internal energies, since system (35) involves relaxation terms in the energy equation. Again, combination of the mass, momentum and energy equations and exact integration yields

$$e_k^* = e_{k0} + \tfrac{1}{2}(u_k^* - u_{k0})^2. \tag{37}$$

We now examine the pressure relaxation step for an arbitrary number of fluids.

https://doi.org/10.1017/S0022112000003098 Published online by Cambridge University Press

3.2.2. *Pressure relaxation operator*

We have proposed in Saurel & Abgrall (1999*a*) a procedure valid only for two fluids. Here, we improve the accuracy of the relaxation pressure step and generalize it to an arbitrary number of fluids. This is important for example for detonation interaction with neighbouring materials. The explosive is considered at least as a mixture of solid and gas, and the neighbouring material is another fluid with an interface that is solved with its own PDE system.

For any phase k we have to solve the ODE system

$$\left.\begin{aligned} \frac{\partial \alpha_k}{\partial t} &= \mu(P_k - P_{k'}), \\ \frac{\partial \alpha_k \rho_k}{\partial t} &= 0, \\ \frac{\partial \alpha_k \rho_k u_k}{\partial t} &= 0, \\ \frac{\partial \alpha_k \rho_k E_k}{\partial t} &= -\mu P_i (P_k - P_{k'}), \end{aligned}\right\} \tag{38}$$

where the relaxation coefficient μ tends to infinity.

Combination of the volume fraction, mass, momentum and energy equations yields

$$\alpha_k \rho_k \frac{\partial e_k}{\partial t} = -P_i \frac{\partial \alpha_k}{\partial t}$$

where P_i is given by equation (12). Note that the first law of thermodynamics is recovered here. Since $m_k = \alpha_k \rho_k = \text{const.}$ then $\mathrm{d}\alpha_k = -m_k \mathrm{d}\rho_k / {\rho_k}^2$. The energy equation becomes:

$$\frac{\partial e_k}{\partial t} = P_i \frac{\partial (1/\rho_k)}{\partial t}.$$

Now, under the trapezoidal approximation: $e_k^* - e_k^0 = (P_i^* + P_i^0)/2(1/\rho_k^* - 1/\rho_k^0)$, where variables marked with an asterisk are relaxed ones, and variables marked with 0 are obtained from the velocity relaxation step.

This corresponds to N equations (N is the number of fluids) with $2N+1$ unknowns: N energies, N densities and P_i^*. When the relaxation parameter tends to infinity, all pressures must be equal: $P_k^* = P_{k'}^* = P_i^*$. So there is only one pressure to determine. To close the system we also have N equations of state: $e_k^* = e_k(P_i^*, \rho_k^*)$. The saturation constraint $\sum \alpha_k = 1$ provides the last equation. The system to solve now is (we suppress the symbol *)

$$\left.\begin{aligned} &2\rho_1 \rho_1^0 (e_1 - e_1^0) + (P_i + P_i^0)(\rho_1 - \rho_1^0) = 0, \\ &2\rho_2 \rho_2^0 (e_2 - e_2^0) + (P_i + P_i^0)(\rho_2 - \rho_2^0) = 0, \\ &\cdots \\ &2\rho_N \rho_N^0 (e_N - e_N^0) + (P_i + P_i^0)(\rho_N - \rho_N^0) = 0, \\ &\sum m_k/\rho_k - 1 = 0. \end{aligned}\right\} \tag{39}$$

The solution of this nonlinear system is obtained with the Newton–Raphson method.

https://doi.org/10.1017/S0022112000003098 Published online by Cambridge University Press

We set $\boldsymbol{X} = (\rho_1, \ldots, \rho_N, P_i)^T$ and

$$\boldsymbol{F}(\boldsymbol{X}) = \begin{pmatrix} 2\rho_1\rho_1^0(e_1 - e_1^0) + (P_i + P_i^0)(\rho_1 - \rho_1^0) \\ \cdots \\ 2\rho_N\rho_N^0(e_N - e_N^0) + (P_i + P_i^0)(\rho_N - \rho_N^0) \\ \sum m_k/\rho_k - 1 \end{pmatrix}.$$

Newton's method gives $\boldsymbol{D}(\boldsymbol{X}^{l-1})\Delta\boldsymbol{X}^l = -F(\boldsymbol{X}^{l-1})$ where l designates the current iteration and $\Delta\boldsymbol{X}^l = (\boldsymbol{X}^l - \boldsymbol{X}^{l-1})$. A solution is obtained when $\Delta X^l < \epsilon$. $\boldsymbol{D}(\boldsymbol{X})$ represents the Jacobian matrix of the nonlinear system ($\boldsymbol{D}(\boldsymbol{X}) = \partial\boldsymbol{F}(\boldsymbol{X})/\partial\boldsymbol{X}$) and is given by

$$\boldsymbol{D}(\boldsymbol{X}) = \begin{pmatrix} A_1 & 0 \cdots & 0 & B_1 \\ & \ddots & & \vdots \\ & & A_N & B_N \\ m_1/\rho_1 & \cdots & m_N/\rho_N & 0 \end{pmatrix}$$

with

$$A_k = 2\rho_k^0(e_k - e_k^0) + 2\rho_k\rho_k^0(e_{k_\rho})_P + (P_i + P_i^0)\rho_k$$

and

$$B_k = 2\rho_k\rho_k^0(e_{k_P})_\rho + (\rho_k - \rho_k^0).$$

This procedure is robust and accurate. It is used in all test problems of the next section.

4. Test problems

We consider here test problems involving interfaces, cavitation, shock and detonations in one and two space dimensions. All test problems involve instantaneous pressure and velocity relaxation. Other test problems with finite rate relaxation (two velocities) and other applications are available in Saurel & Abgrall (1999*a*).

4.1. *Interface test problems*

4.1.1. *Water–air shock tube*

We consider a shock tube filled on the left side with high-pressure liquid water and on the right side with air. This test problem consists of a conventional shock tube with two fluids and possesses an exact solution. For this test problem, standard methods based on the Euler equations fail at the second time step.

Each fluid is governed by the stiffened gas equation of state (Godunov *et al.* 1979):

$$P = (\gamma - 1)\rho e - \gamma P_{inf} \tag{40}$$

where γ and P_{inf} are constant parameters. The initial data are: $\rho_l = 1000\,\mathrm{kg\,m^{-3}}$, $P_l = 10^9\,\mathrm{Pa}$, $u_l = 0\,\mathrm{m\,s^{-1}}$, $\gamma_l = 4.4$, $P_{inf_l} = 6 \times 10^8\,\mathrm{Pa}$, $\alpha_l = 1 - \epsilon(\epsilon = 10^{-6})$ if $x < 0.7$; $\rho_g = 50\,\mathrm{kg\,m^{-3}}$, $P_g = 10^5\,\mathrm{Pa}$, $u_g = 0\,\mathrm{m\,s^{-1}}$, $\gamma_g = 1.4$, $P_{inf_g} = 0$, $\alpha_g = 1 - \epsilon$ otherwise. To show mesh convergence of the results, a mesh involving 1000 cells is used. The corresponding results are shown on figure 1 at time 229 ms. For this test case, the right and left chambers contain nearly pure fluids: the volume fraction of gas in the water chamber is only 10^{-6} and vice versa in the gas chamber. The phase densities and internal energies are not compared with the exact solution because no exact solution exists for these variables (no exact Riemann solver is available for this model). But

https://doi.org/10.1017/S0022112000003098 Published online by Cambridge University Press

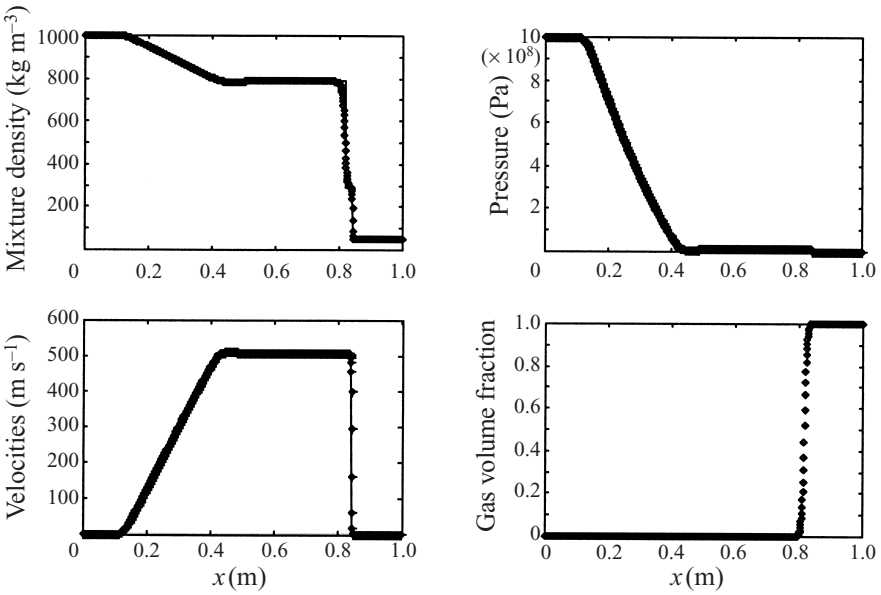

FIGURE 1. Water–air shock tube. Computed solution with 1000 cells (symbols) and exact solution (lines).

the mixture density, the phase pressures and velocities can be compared with the exact solution. The graphs for the pressures and velocities show three curves: two numerical curves and the exact solution. The two curves representing gas and liquid pressure and velocities are indiscernible. This is a result of the pressure and velocities relaxation procedures that give an accurate relaxed state. The mixture density is obtained by a combination of the phase densities that are weighted by the volume fraction and summed.

The graph representing the mixture density shows an excessive numerical diffusion of the interface. This is a result of the stiffness of this problem. The two materials, air and water, have a very different behaviour and EOS parameters, and the pressure ratio is too high (see the pressure graph). This situation for the liquid phase is close to one where the liquid should be connected to a vacuum. Also, the excessive numerical diffusion is a result of our approximate Riemann solver. This is clearly visible on figure 2 where a mesh with only 100 cells is used.

The Riemann solver uses only the two fastest waves instead of the total number of waves (seven here). This will be remedied in the future Abgrall & Saurel (2000).

4.1.2. *Two-dimensional water–air shock tube*

We now consider the same type of problem in two dimensions. The liquid and gas are initially at the same conditions as in the previous test problem. A high-pressure liquid square is located at the centre of the domain as shown on figure 3. The liquid contains 1% gas and vice versa. Results are shown at time 0.1 m s on the same figure. The volume fraction contours show two gradient zones. The external one represents the gas–liquid interface. The inner one represents cavitation effects inside the liquid. Because of the pressure differential, the interface first expands as in the one-dimensional shock tube. Then the two-dimensional rarefaction waves interact and reflect at the centre of the domain resulting in an over-expansion of the liquid. Inertial effects and rarefaction wave focusing produce liquid densities outside the

https://doi.org/10.1017/S0022112000003098 Published online by Cambridge University Press

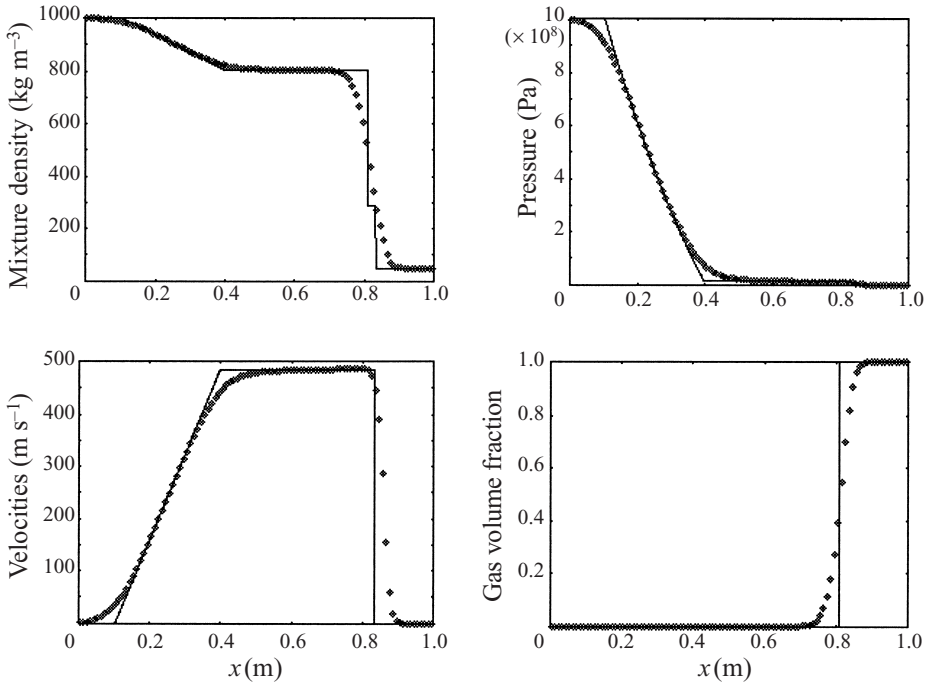

FIGURE 2. Water–air shock tube. Computed solution with 100 cells (symbols) and exact solution (lines).

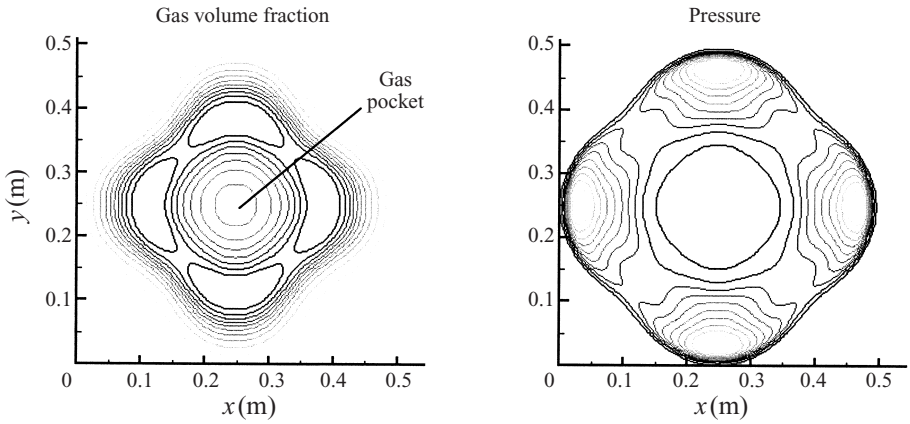

FIGURE 3. Two-dimensional water–air shock tube. Volume fraction gradients indicate the interface and cavitation zones. The pressure remains always positive.

domain of validity of the equation of state of pure liquid. In other words, if this type of computation is done with single-phase equations (i.e. Euler), the pressure becomes negative, even if a very accurate method is used for the computation of the interface. Here, with the multiphase model, rarefaction effects induce gas or bubble expansion instead of liquid and the pressure remains positive. This is closer to reality when mass transfer appears in liquid to form vapour. In this computation, mass transfer is not active, and gas expansion is only due to pressure relaxation.

Cavitation and dynamic interface creation are more visible on the next examples.

https://doi.org/10.1017/S0022112000003098 Published online by Cambridge University Press

4.2. *Cavitation test problems*

4.2.1. *One-dimensional cavitation tube*

Consider a tube filled with water and imagine that the right part is set in motion to the right, and the left part is set in motion in the opposite direction. In such a situation, the pressure, the density and the internal energy decrease across the rarefaction waves in order that the velocity reaches zero at the centre of the domain. The pressure decreases until it reaches the saturation pressure at the local temperature. When the saturation pressure is reached mass transfer appears and part of the liquid becomes gas: the flow becomes a two-phase mixture.

When this type of problem is solved with the Euler equations, so with a single-fluid model and an appropriate equation of state for the liquid (the stiffened gas EOS for example), the pressure becomes completely wrong (i.e. negative). The reason is that the stiffened gas EOS, like any equation of state for liquids and solids, is no longer valid when mass transfer occurs. Indeed the liquid transforms to gas, and the gas is governed by a very different EOS.

There are two alternative ways to solve this problem. The first one is to construct an EOS valid for the liquid phase, the two-phase mixture, and the gas phase. Such a type of approach is taken when the Euler equations are solved with the van der Waals (or other) equation of state. But it has been shown (Godunov *et al.* 1979; Menikoff & Plohr 1989) that convexity of the EOS was necessary for well-posedness. Clearly, the requirement is not satisfied with the van der Waals and other cubic EOS. Another type of EOS that avoids this problem is derived in Saurel *et al.* (1999). But this model EOS assumes that mass transfer occurs at an infinite rate. This is not always correct.

The second alternative is to use the non-equilibrium multiphase flow model. With this model, each phase possesses its own EOS and proper behaviour. The liquid phase will be governed by the stiffened gas EOS, and the gas phase by the ideal gas one.

To model cavitation, mass transfer effects need to be considered. But to introduce it, relations (17)–(20) can be used with a given correlation for the energy transfer (19). Clearly, there are strong uncertainties about these correlations in cavitating flows. So, we prefer to not consider mass transfer but to examine the model behaviour in a simplified situation where a small fraction of gas is initially present in the liquid (1% gas by volume). From this initial situation where the gas and liquid are at atmospheric pressure, we set into motion the right part of the tube at $100\,\mathrm{m\,s^{-1}}$, and the left part at $-100\,\mathrm{m\,s^{-1}}$. The results are shown on figure 4.

The density graphs show the liquid and gas evolutions. The liquid density decreases slightly but remains close to the initial one. The liquid remains liquid at a positive pressure. The gas density decreases across the rarefaction waves and decreases again due to the pressure relaxation process. The gas density at the centre of the tube is very low. The pressure relaxation process makes the gas volume fraction increase. So, the mixture density decreases too, as expected, and the velocity profiles tend to the expected solution. It is important to note that the increase in gas volume fraction creates two interfaces propagating to the right and to the left. So this method has the capability of creating dynamically interfaces starting from a nearly pure liquid. This feature has important applications for specific problems, as shown on the following two-dimensional example.

4.2.2. *Two-dimensional cavitation around an obstacle in a supersonic liquid flow*

The following two-dimensional, unsteady calculation is done with the same mixture as previously: 99% water and 1% gas at atmospheric pressure and temperature,

https://doi.org/10.1017/S0022112000003098 Published online by Cambridge University Press

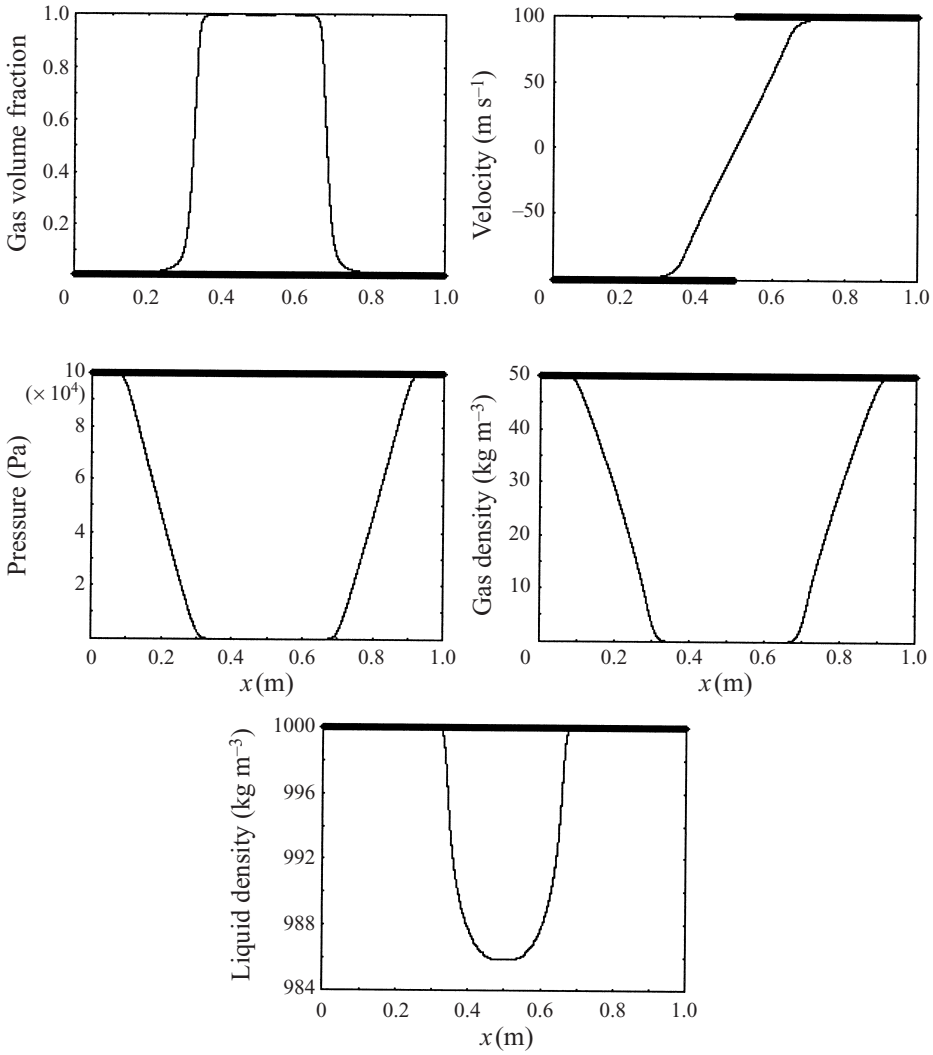

FIGURE 4. One-dimensional cavitation tube. Interfaces appear dynamically, pressure remains positive and liquid density remains inside the domain of validity of the EOS. The numerical solution is shown at time 1826 μs with thin lines. The initial condition is represented with thick lines.

flowing over an obstacle with a given inflow velocity. The obstacle surface is treated as a rigid wall with centreline symmetry. The outflow and upstream boundaries are treated as non-reflecting. At the inflow boundary on the left-hand side the fluid is 99% liquid and 1% gas moving at 2000 m s^{-1} (supersonic relative to the liquid sound speed). The obstacle has conical-shaped leading and trailing edges and a cylindrical centrebody. Since the inflow is supersonic, a detached shock wave is expected in front of the obstacle as represented on the pressure contours in figure 5. On the two angular points connecting the cones to the cylindrical portion, strong rarefaction waves are expected, possibly capable of inducing cavitation. Volume fraction contours are presented in figure 5(*a–c*) at 1, 10 and 20 μs to illustrate the unsteady formation of cavitation pockets and bubble tearing. Figure 5(*d*) shows the pressure contours. The detached shock wave in front of the obstacle is clearly visible.

https://doi.org/10.1017/S0022112000003098 Published online by Cambridge University Press

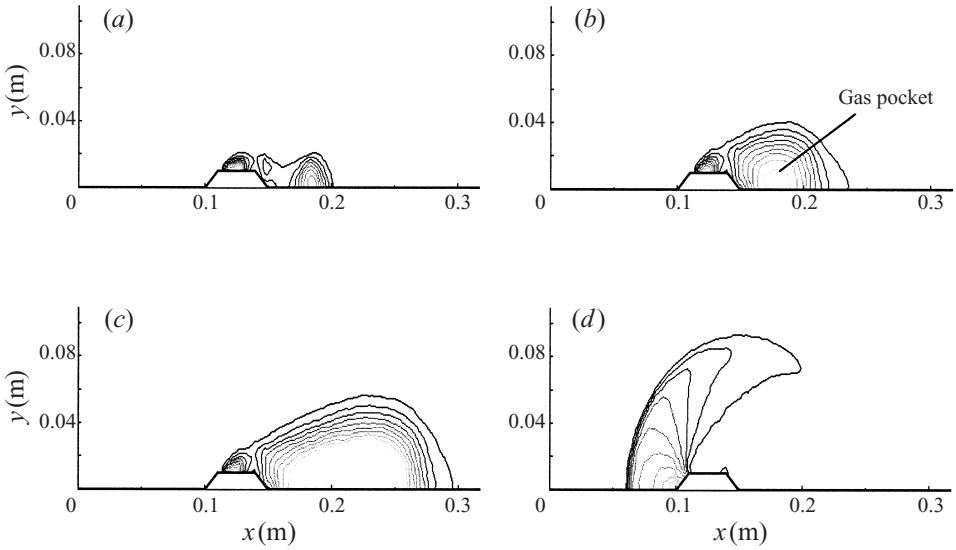

FIGURE 5. Two-dimensional supersonic liquid flow around a cylindrical projectile. Cavitation pockets appear dynamically. (a, b, c) Gas volume fraction at $t = 1\,\mu s$, $10\,\mu s$ and $20\,\mu s$ respectively; (d) pressure at $t = 10\,\mu s$.

4.3. *Shock and detonation test problems*

4.3.1. *Shock propagation in solid alloys*

We now evaluate the model and method capabilities for the computation of shock waves in a two-phase mixture for a test problem involving very strong shock waves. The two-phase system does not admit conventional Rankine–Hugoniot relations because non-conservative and relaxation terms are present in the equations. But it is possible to solve these equations in the unsteady regime with the proposed numerical method, and to examine the two-phase shock wave behaviour. To do this, we simulate the impact of a piston on two-phase mixtures. The piston impact is treated as a boundary condition. In order to evaluate computed results, we need reference solutions. Specific situations with experimental results are available in the literature. Indeed, for many solid alloys the Hugoniot curve is available. These experimental data relate the shock velocity U_s to the material velocity u: $U_s = c_0 + su$ where c_0 is the material sound speed under atmospheric conditions and s a dimensionless constant.

Under very strong impact conditions, as is usual with shocks in solids and detonation applications, the solids are of course compressible and behave like fluids. In these conditions a solid alloy is simply a multiphase or multifluid solid mixture. So, to obtain the numerical Hugoniot curve of the alloy we compute with the multiphase model several unsteady impact problems, by varying the velocity boundary condition, and we note the shock velocity versus the impact (material) velocity. We obtain the results shown in figure 6. Part(a) is related to brass (Cu/Zn alloy), with an initial zinc volume fraction of 0.29. Figure 6(b) is related to a uranium/rhodium alloy with an initial rhodium volume fraction of 0.265. Figure 6(a) corresponds to an epoxy/spinel mixture, with an initial epoxy volume fraction of 0.595.

On each graph, the experimental data are represented with symbols. The curves represent two different theoretical approaches. The first one, which fits correctly the experimental data, is obtained with the multiphase model. This model needs only the pure material equations of state for each substance, which are well known. The second

https://doi.org/10.1017/S0022112000003098 Published online by Cambridge University Press

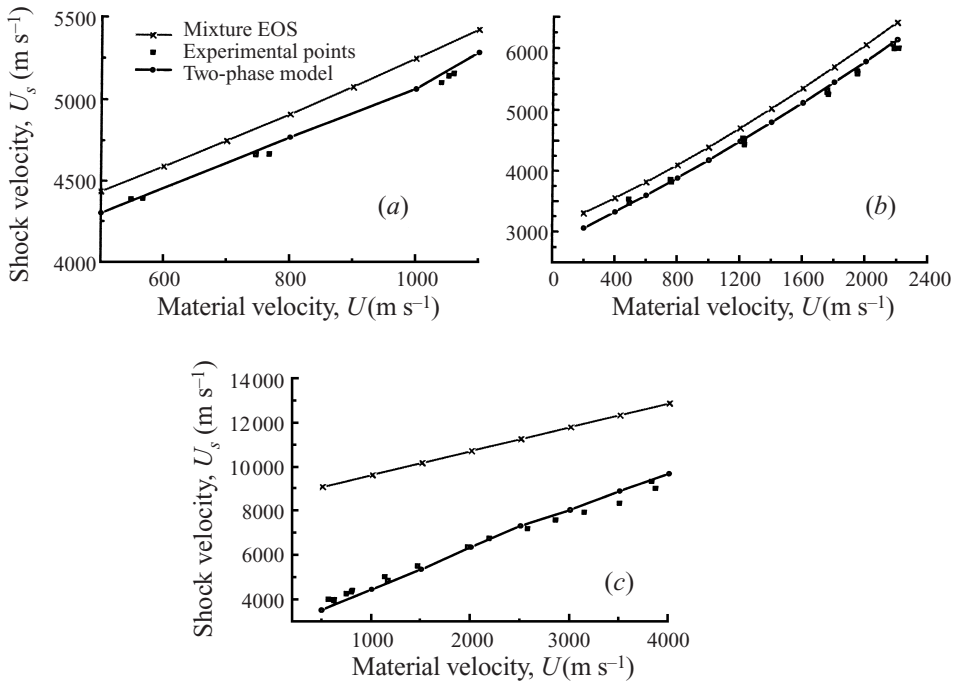

FIGURE 6. Experimental and theoretical Hugoniot curve for several alloys: (*a*) Cu/Zn, (*b*) U/rhodium, (*c*) epoxy/spinel. The numerical Hugoniot from multiphase computation fits correctly experimental data.

one is the conventional approach, based on the Euler equations with an equation of state for the mixture. This type of procedure is described for example in Massoni *et al.* (1999) and Shyue (1998). The errors induced by the mixture equations of state are clearly visible here. This analysis demonstrates the advantage of the multiphase flow approach for such problems.

4.3.2. *Detonation waves and mixture equation of state*

We evaluate here the capabilities of the method to compute detonation waves in solid energetic materials. Unlike the previous test problem, it now involves mass and energy transfers. Some care must be taken with the numerical method in such a situation. When the mass transfer effects are considered in the presence of a shock wave, the non-conservative terms $P(\partial\alpha/\partial x)$ and $Pu(\partial\alpha/\partial x)$ may pose some difficulty. Indeed, the numerical approximation for $\partial\alpha/\partial x$ has been derived for a specific situation where P and u were uniform and α discontinuous. When dealing with shock waves, P and u are discontinuous but α is constant (or nearly). Thus, the numerical approximation of $P(\partial\alpha/\partial x)$ does not pose any problem. But when dealing with detonation waves, α is no longer constant because of mass transfer. The solution we have adopted to avoid this problem is to forbid mass transfer inside the shock. To detect the shock front we use the following shock indicator: when $P_i^{n+1}/P_i^n > 1+TOL$ where TOL represents a given tolerance (0.2 for practical computations), then the mesh point i lies inside the shock front. This numerical treatment is in agreement with the detonation structure.

Another numerical approach to deal with the problem of shocks, as well as with the problem of smeared interfaces, is developed in a work in progress (Abgrall &

https://doi.org/10.1017/S0022112000003098 Published online by Cambridge University Press

Saurel 2000). The multiphase model is particularly interesting for detonation wave modelling for the following reason. With solid explosives, inside the reaction zone it is reasonable to think that the solid retains a grain shape structure at the microscopic scale. The typical size of solid elemental particles will be much bigger than the size of a molecule. So, even if molecular collisions and turbulence effects are present, they will not induce temperature equilibrium in the mixture. With the multiphase model each phase possesses its own temperature and density.

For the following test problem, we show that our model and method furnishes the correct solution for detonation waves, and also that temperature and densities are always out of equilibrium inside the reaction zone.

In order to compare the solution of the multiphase model to an exact solution we choose an unusual test problem. We consider that the solid and the gas phase are governed by the same equation of state, and to simplify the analysis we chose the ideal gas equation of state $P = (\gamma - 1)\rho e$ with $\gamma = 3$ for both phases. Then, the multiphase model solution must degenerate to the single-phase Euler solution for all mixture variables.

Inside the detonation wave reaction zone the reactive Euler equation can be solved exactly between the shock point (Neumann spike) and the point moving at the sonic velocity relative to the shock front (CJ point). This conventional calculation corresponds to the ZND model solution and can be performed exactly in a simplified situation such as given in Fickett & Davis (1979), or by the resolution of an ODE problem with a nearly exact accuracy. Here, we use the conditions of the ZND problem given in Fickett & Davis.

We use exactly the same explosive data and we solve the entire flow in the unsteady regime. After the shock-to-detonation transition a stable detonation wave is obtained. When this detonation is stable (the bottom curves of figures 7) we compare the reaction zone obtained from the computation and the exact solution. Comparison is made only in the reaction zone because the ZND model is valid only in this part. Also, comparison is possible only for mixture flow variables: the ZND problem has never been solved for multiphase mixtures. Results are shown in figure 7. The exact solution is shown with symbols and the numerical one is plotted with lines. Results are shown at time 12.11 μs. The thick lines are related to the solid phase variables and the thin ones to the gas phase. It appears that the numerical solution converges to the exact one. The other important result is that the densities and temperatures of the two fluids are never in equilibrium inside the reaction zone, even for this basic test problem where the equation of state and material properties are exactly the same. This result is actually obvious: the gas phase receives energy from the solid phase, while the solid phase does not receive any energy.

Some spurious oscillations are visible on the curves near $x = 0$. The oscillation in the mixture density and phase temperature is due to the overheating phenomena (Fedkiw *et al.* 1999). The unrealistic level reached by the solid-phase density near the location $x = 0$ is a combination of overheating and mass transfer. Indeed, at this location, the solid phase is no longer present: the solid volume fraction is nearly zero and the solid density calculation has no physical meaning.

5. Conclusion

A compressible multiphase unconditionally hyperbolic model has been proposed. It is able to deal with a wide range of applications: interfaces between compressible

https://doi.org/10.1017/S0022112000003098 Published online by Cambridge University Press

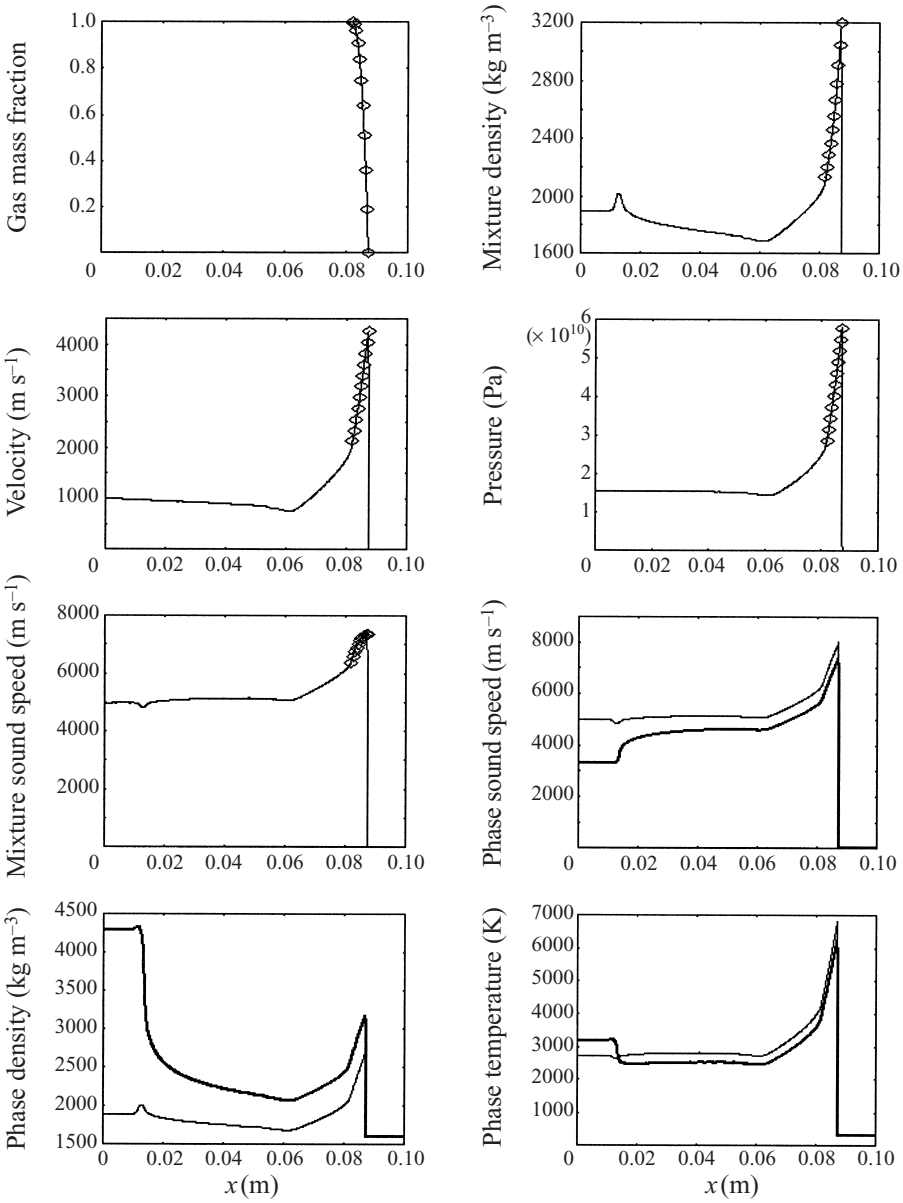

FIGURE 7. Detonation test problems. Mixture variables are compared to ZND calculation inside the reaction zone. Results show that fluid temperatures and densities are never in equilibrium.

materials, shock waves in condensed multiphase mixtures, homogeneous two-phase flows (bubbly and droplet flows) and cavitation in liquids. It is able to create dynamically interfaces in cavitating flows, and to deal with mutiphase mixtures as well as interface problems.

This model does not need a mixture equation of state and provides thermodynamic variables for each phase. This is important for detonation modelling. Also, it is conservative regarding the mixture, even at the interfaces. This provides accurate energy and temperature computation.

https://doi.org/10.1017/S0022112000003098 Published online by Cambridge University Press

The authors are particularly grateful to Gerard Baudin (CEG), Serge Gauthier and Francois Renaud (CEA Bruyères le Chatel), Lionel Sainsaulieu and Fabienne Galzin (RENAULT) and Robert Belmas (CEA Le Ripault). They also address special thanks to Jacques Massoni, Ashwin Chinnayya and Eric Daniel for their daily support.

REFERENCES

Abgrall, R. 1996 How to prevent pressure oscillations in multicomponent flow calculations: A quasi conservative approach. *J. Comput. Phys.* **125**, 150–160.

Abgrall, R., Nkonga, B. & Saurel, R. 2000 Efficient numerical approximation of compressible multi-material flow for unstructured meshes. Submitted to *Computers Fluids.*

Abgrall, R. & Saurel, R. 2000 A numerical multiphase model. In preparation.

Baer, M. R. & Nunziato, J. W. 1986 A two-phase mixture theory for the deflagration-to-detonation transition (DDT) in reactive granular materials. *Intl J. Multiphase Flows* **12**, 861–889.

Benson, D. J. 1992 Computational methods in Lagrangian and Eulerian hydrocodes. *Comput. Meth. Appl. Mech. Engng* **99**, 235–394.

Bestion, D. 1990 The physical closure laws in the CATHARE code. *Nucl. Engng Design* **124**, 229–245.

Butler, P. B., Lambeck, M. F. & Krier, H. 1982 Modelling of shock development and transition to detonation initiated by burning in porous propellant beds. *Combust. Flame* **46**, 75–93.

Byrne, G. D. & Dean, A. M. 1992 The solution of co-polymerization problems with VODE. In *Recent Developments in Numerical Methods for ODE's/DAE's/PDE's* (ed. G. D. Byrne & Schiesser), pp. 137–197. World Scientific.

Cocchi, J. P. & Saurel, R. 1997 A Riemann problem based method for compressible multifluid flows. *J. Comput. Phys.* **137**, 265–298.

Dervieux, A. & Thomasset, F. 1981 Multifluid incompressible flows by a finite element method. Lecture Notes in Physics, vol. 141, pp. 158–163. Springer.

Drew, D. A. & Passman, S. L. 1998 *Theory of Multicomponent Fluids.* Springer.

Farhat, C. & Roux, F. X. 1991 A method for finite element tearing and interconnecting and its parallel solution algorithm. *Intl J. Numer. Math. Engng* **32**, 1205–1227.

Fedkiw, R. P., Aslam, T., Merriman, B. & Osher, S. 1999 A non oscillatory eulerian approach to interfaces in multimaterial flows (The Ghost Fluid Method). *J. Comput. Phys.* **152**, 457–492.

Fedkiw, R. P., Marquina, A. & Merriman, B. 1999 An isobaric fix for the overheating problem in multimaterial compressible flows. *J. Comput. Phys.* **148**, 545–578.

Fickett, W. & Davis, W. C. 1979 *Detonation.* University of California Press, Berkeley.

Gavrilyuk, S. & Saurel, R. 2000 A compressible multiphase model with microinertia. Submitted to *J. Comput. Phys.*

Glimm, J., Grove, J. W., Li, X. L., Shyue, K. M., Zhang, Q. & Zeng, Y. 1998 Three dimensional front tracking. *SIAM J. Sci. Comput.* **19**, 703–727.

Godunov, S. K. 1959 A finite difference method for the numerical computation of discontinuous solutions of the equations of fluid dynamics. *Math. Sb.* **47**, 357–393.

Godunov S. K., Zabrodine, A., Ivanov, M., Kraiko, A. & Prokopov, G. 1979 *Résolution Numérique des Problèmes Multidimensionnels de la Dynamique des Gaz.* Editions Mir, Moscou.

Harten, A. & Hyman, M. J. 1983 Self adjusting grid methods for one-dimensional hyperbolic conservation laws. *J. Comput. Phys.* **50**, 235–269.

Harten, A., Lax, P. D. & Leer, B. van 1983 On upstream differencing and Godunov type schemes for hyperbolic conservation laws. *SIAM Rev.* **25**, 33–61.

Hirt, C. W. & Nichols, B. D. 1981 Volume Of Fluid (VOF) method for the dynamics of free boundaries. *J. Comput. Phys.* **39**, 201–255.

Jouëtte, C. de, Laget, O., Le Gouez, J. M. & Rigaud, S. 1997 Résistance à l'avancement des navires rapides par une methode 'Volume of Fluids' (VOF). *6eme Journeés de l'Hydrodynamique. Ecole Centrale de Nantes.* ISSN 1161-1847.

Kapila, A., Son, S., Bdzil, J., Menikoff, R. & Stewart, D. 1997 Two-phase modeling of DDT: structure of the velocity-relaxation zone. *Phys. Fluids* **9**, 3885–3897.

Karni, S. 1994 Multicomponent flow calculations by a consistent primitive algorithm. *J. Comp. Phys.* **112**, 31–43

https://doi.org/10.1017/S0022112000003098 Published online by Cambridge University Press

Karni, S. 1996 Hybrid multifluid algorithms. *SIAM J. Sci. Comput.* **17**, 1019–1039.

Kolev, N. I. 1993 Fragmentation and coalescence dynamics in multiphase flows. *Exptl Therm. Fluid Sci.* **6**, 211–251.

Kuo, K. K., Yang, V. & Moore, B. B. 1980 Intergranular stress, particle-wall friction and speed of sound in granular propellant beds. *J. Ballistics* **4**, 697–730.

Leer, B. van 1979 Toward the ultimate conservative difference scheme. V. A second order sequel to Godunov's Method. *J. Comput. Phys.* **32**, 101.

Leveque, R. J. & Shyue, K. M. 1996 Two-dimensional front tracking based on high resolution wave propagation methods. *J. Comput. Phys.* **123**, 354–368.

Liou, M. S. & Edwards, J. R. 1999 AUSM schemes and extensions for low Mach and multiphase flows. *Lect. Series 1999–03, 30th Computational Fluid Dynamics, March 8–12, 1999*. von Karman Institute for Fluid Dynamics.

Mao, D. K. 1993 A treatment of discontinuities for finite difference methods in two dimensional case. *J. Comput. Phys.* **104**, 235–269.

Massoni, J., Saurel, R., Baudin, G. & Demol, G. 1999 A mechanistic model for shock initiation of solid explosives. *Phys. Fluids* **11**, 710–736.

Massoni, J., Saurel, R., Nkonga, B. & Abgrall, R. 2000 Proposition de méthodes et modèles euleriens pour les problèmes à interfaces entre fluides compressibles en presence de transfert de chaleur. *Submitted to Intl J. Heat Mass Transfer*.

Mazel, P., Saurel, R., Loraud, J. C. & Butler, P. B. 1996 A numerical study of weak shock wave propagation in a reactive bubbly liquid. *Shock Waves* **6**, 287–300.

Menikoff, R. & Plohr, B. J. 1989 The Riemann problem for fluid flows of real materials. *Rev. Mod. Phys.* **61**, 75–130.

Mitani, T. & Williams, F. A. 1986 A model for the deflagration of nitramines. *Sandia Natl Lab. Rep.* SAND86-8230. Livermore, CA.

Molin, B., Dieval, L., Marcer, R. & Arnaud, M. 1997 Modélisation instationnaire de poches de cavitation par la méthode VOF. *6eme Journees de l'Hydrodynamique. Ecole Centrale de Nantes.* ISSN 1161-1847.

Morel, C., Goreaud, N. & Delhaye, J. M. 1999 The local volumetric interfacial area transport equation: derivation and physical significance. *Intl J. Multiphase Flows*, to appear.

Mulder, W., Osher, S. & Sethian, J. A. 1992 Computing interface motion: The compressible Rayleigh-Taylor and Kelvin-Helmoltz instabilities. *J. Comput. Phys.* **100**, 209.

Powers, J. M., Stewart, D. S. & Krier, H. K. 1990 Theory of two-phase detonation–Part I: modeling. *Combust. Flame* **80**, 264.

Rowe, P. N. 1961 Drag forces in a hydraulic model of fluidized bed. Part II. *Trans. Inst. Chem. Engrs* **39**, 175–180.

Sainsaulieu, L. 1995 Finite volume approximations of two phase fluid flows based on an approximate Roe-type Riemann solver. *J. Comput. Phys.* **121**, 1–28.

Saurel, R., Larini, M. & Loraud, J. C. 1992 Ignition and growth of a detonation by a high energy plasma. *Shock Waves* **2(1)**, 91–102.

Saurel, R. 1996 Numerical analysis of Ram Accelerator employing two-phase combustion. *AIAA J. Prop. Power* **12**, 708–717.

Saurel, R. & Abgrall, R. 1999*a* A multiphase Godunov method for compressible multifluid and multiphase flows. *J. Comput. Phys.* **150**, 425–467.

Saurel, R. & Abgrall, R. 1999*b* A simple method for compressible multifluid flows. *SIAM J. Sci. Comput.* **21**, 1115–1145.

Saurel, R., Cocchi, J. P. & Butler, P. B. 1999 A numerical study of the cavitation effects in the wake of a hypervelocity underwater projectile. *AIAA J. Prop. Power* **15**, 513–522.

Saurel, R. & Mencacci, S. 1999 HYDRO3D: un outil simple pour la simulation de problèmes de détonique. *7e Congrés Intl de Pyrotechnie, Europyro 99, Brest, 7–11 juin 1999*.

Shyue, K. M. 1998 An efficient shock-capturing algorithm for compressible multicomponent problems. *J. Comput. Phys.* **142**, 208.

Strang, G. 1968 On the construction and comparison of difference schemes. *SIAM J. Numer. Anal.* **5**, 506–517.

Tan, M. J. & Bankoff, S. G. 1984 Propagation of pressure waves in bubbly mixtures. *Phys. Fluids* **27**, 1362–1369.

Toro, E. F. 1989 Riemann-Problem based techniques for computing reactive two-phase flows. In

https://doi.org/10.1017/S0022112000003098 Published online by Cambridge University Press

Proc. Third. Intl Conf. on Numerical Combustion (ed. Dervieux & Larrouturrou). Lecture notes in Physics, vol. 351, pp. 472–481. Antibes, France.

Toro, E. F. 1997 *Riemann Solvers and Numerical Methods for Fluid Dynamics*. Springer.

Utheza, F., Saurel, R., Daniel, E. & Loraud, J. C. 1996 Droplet breackup through an oblique shock wave. *Shock Waves* **5**, 265–273.

Wijngaarden, L. van 1972 One-dimensional flow of liquids containing small gas bubbles. *Ann. Rev. Fluid Mech.* **4**, 369–396.

Youngs, D. L. 1982 Time dependent multi-material flow with large fluid distortion (ed. K. W. Morton & M. J. Baines). Academic.

Yuen, M. C. & Chen, L. W. 1977 Heat transfer measurements of evaporating liquid droplets. *Intl J. Heat Mass Transfer* **21**, 537–542.

https://doi.org/10.1017/S0022112000003098 Published online by Cambridge University Press